DESIGN AND ANALYSIS OF A METAMATERIAL

WITH HIGH REFRACTIVE INDEX AT

DUAL BAND FREQUENCIES

_____

A Thesis

presented to

the Faculty of the Graduate School

at the University of Missouri-Columbia

_____

In Partial Fulfillment

of the Requirements for the Degree

Master of Science

_____

by

ZAN LU

Dr. Naz. E. Islam, Thesis Supervisor

DECEMBER 2012

The undersigned, appointed by the dean of the Graduate School, have examined the [thesis or dissertation] entitled

DESIGN AND ANALYSIS OF A METAMATERIAL

WITH HIGH REFRACTIVE INDEX AT

DUAL BAND FREQUENCIES

presented by Zan Lu,

a candidate for the degree of [master of science],

and hereby certify that, in their opinion, it is worthy of acceptance.

Professor Naz Islam

Professor Mahmoud Almasri

Professor H. R. Chandrasekhar

ACKNOWLEDGEMENTS

Here I would like to give my special thank my advisor Dr. Naz Islam, who provide me the research opportunity in his high power electromagnetic research lab and who provides me the idea and direction for my research on the novel topic of metamaterials. I would also like to thank Dr. Mahmoud Almasri and Dr. H. R. Chandrasekhar as my thesis committee members providing me remarkable comments and suggestions on my research.

Thanks to all my lab members who has left and who's still working in the lab. They helped me to start to use the software and then provide me some creative ideas during my research. With their support, I managed to get over all the difficulties on the path of my research and with their support I spent a really meaningful life in the lab.

Finally, I want to thank my parent, my grandma, my auntie and my sister who are always loving me and supporting me to the end. Without their love, I might not have achieved so far.

TABLE OF CONTENTS

LIST OF FIGURES

vii

LIST OF TABLES

ABSTRACT

The study and design of metamaterials that produces high refractive index values at different operating frequencies is important since this material parameter has applications in imaging, lithography, compact optical circuits, and miniaturized electromagnetic devices. Resolutions vary inversely with refractive index values.

Research and developments in recent years have demonstrated the design of a single frequency band, single high-refractive-index metamaterials. In this research the concept of single frequency, single refractive material has been extended with the design of dual frequency band, dual high-refractive-index metamaterials in the THz regime. Analysis show that higher refractive index at the second resonance frequency band is achievable through redesign of the structures. The designed structure consists of twenty five unit-cells with a surface area of 250 um by 250 um and a thickness of 5 um. Each cell has metallic structures embedded in a polyimide substrate. Analysis show strong electrical responses at two frequency range and the extracted constitutive parameters suggested high values of simultaneous dielectric constant, permeability and refractive indices.

The structures were also studied with changing unit cell parameters such the area, thickness and the dimensions of embedded structures, including their separation distances. Analysis shows that further modifications of the unit cell could lead to the design of a single structure having more than two high-refractive-index values at different frequencies, thus making the structure a commercially viable product for many applications.

Chapter

1. INTRODUCTION: METAMATERIALS

Where does the word "metamaterial" come from?

The Greek word "meta" means beyond or at a higher level [1], relating to change of a state or position. Since the new artificial designed materials introduced by Victor Veselago [2] and J. P. Pendry [3] in the late 60's and early 90's have properties being considered as beyond those of natural occurring materials, the Greek word "meta" is then attached to the word "material" and hence these kind of "supernatural" materials are called metamaterials.

1.1 What are metamaterials?

Metamaterials were first introduced and designed in the 1960's for microwave frequencies as an extension of the concept of the artificially designed dielectric to enhance or even replace the electromagnetic properties of the naturally existing materials. With the development of the fabrication techniques and the broad application of this artificial material, metamaterial has experienced a great boost in its design which attracting more and more interested to researchers and scientists.

A typical metamaterial consists of embedded periodic geometric structures, usually metallic, in a host substrate which is usually a dielectric. From another perspective, the structure as a whole can be seen as a normal homogeneous dielectric structure where its optical property is a result of its nano-scale atoms while the metamaterial owns its property from the subwavelength structure embedded in it. Since the size of the atoms in the homogenous dielectric is much smaller than the wavelength of optical waves, at the wavelength that is much longer than the size of the unit cell of the metamaterial, the metamaterial structure can demonstrate the

1

parameters as those used to describe the homogeneous dielectrics, where the subwavelength unit cells perform as the atoms in the dielectrics. As a result of its flexibility of manipulating its geometry, ease of implementation and its similarity in propagating wave as that of dielectrics, the metamaterial has broaden its application at a fast speed in the microwave frequency range and even optical frequency range..

Just like homogeneous dielectrics that exhibit optical properties such as refractive index, permittivity and permeability to the nanometer-scale of their atoms, metamaterials also derive their own properties from the subwavelength structure of their component materials. At the wavelength that is much larger than the unit cell in a periodic setup, the structure can be described as a homogeneous dielectric and the effective-medium theories allow the characterization of the electromagnetic properties of this composite structure of metamaterials [4]. These properties of the metamaterial depend on a number of factors, including the host materials' property as well as the embedded material property, the volume of the fraction, the operating frequency, and the morphology of the composite material, such as the dimensions and shapes of the host structure and the guest structure. Overall, the properties of metamaterial depend mostly on the properties of the guest material's property and its morphology. So when all other variables are known, the main key to the control the property of the metamaterial is the change of the morphology of the embedded structure, which allows for a wide range of change of the properties of the metamaterial such as the permittivity, permeability and the refractive index value in the desired frequency range.

1.2 Development of metamaterial

Metamaterials, first known as left-handed material (LHM) or negative refractive index material (NIM) and introduced by D. R. Smith in the early 00's [5], has attracted a great deal of attention in the material and optical research communities over the past decade. An early stage of designed metamaterial gave only a single magnetic response or electric response at a specific frequency range with a single tuned permeability or permittivity [6]. However, following the development of the concept, design and application of metamaterials and manufacturing techniques, the definition of metamaterials has been broadened to have a much wider scope than that of left-handed material or negative index material. Due to the broad research on metamaterials, the traditional subjects of electromagnetism and optics have experienced a number of discoveries and changes.

The first concept of metamaterial proposed by Veselago theoretically in 1968 was defined as a material possessing negative electric permittivity and negative magnetic permeability simultaneously at a certain operating frequency range. This so called left-handed material has new features other than the proposed negative permittivity and permeability, such as negative refraction, backward wave propagation, reversed Doppler shift and more. However, research on this novel left-handed material after Veselago's proposal has been sluggish for 30 years due to the lack of verification in experiment and real word test, until when, the first revolution took place in 1996 by a great scientist from British. This year, Dr. Pendry from Imperial College London discovered the wired structure metamaterials with negative permittivity; later in 1999, he discovered the SRR based structure metamaterials with negative permeability. Along with the proposal of these two types of metamaterials, Dr. Pendry

also developed the detailed mathematic procedure for the calculation of and retrieval of the permittivity and permeability, which is based mainly on the dimensional information of the metamaterial. In 2000 Dr. Smith developed the left-handed material [7] with negative refractive index using the theory provided by Dr. Veselago and Dr. Pendry. Inspired by these revolutionary successes in experimental realization of metamaterial or the left-handed material, researchers have experienced a boost in the theoretical and experimental study of it. This incredible boost resulted in a great increase in more discoveries and exploration of the properties of metamaterial which could not have been obtained in naturally existing material and limited to the negative refraction index only.

The next milestone in the development of metamaterials came in 2005 when Dr. Smith discovered that the gradient refractive index medium was able to bend electromagnetic waves in a certain direction through the manipulation of the refractive index [8]. In 2006, invisible cloaks were invented by controlling the propagation of the electromagnetic waves using metamaterials [9]. By then, metamaterials have had a much wider range of definition than that of the original negative refractive index, which opened more areas for research for the metamaterial, including ultrahigh refractive index and near zero refractive. In conclusion it can be said that, the essential principle of metamaterials is the ability to control the electromagnetic properties when interacting with propagating wave by manipulating the morphology of the embedded metallic structure whose dimension is much smaller than the wavelength, and to bring about the desired properties that are not available in the natural materials [10].

In the research presented in this document, the focus is to design and analyze metamaterial with high refractive index by manipulating the geometry of the metallic structure. A specifically designed structure is given with the theoretical analysis of the mechanism of achieving the high refractive index described and the detailed design process is provided. The optimization procedure of the metallic structure is demonstrated while the analysis and discussion is then provided in the final conclusion. In chapter 2, fundamentals of the electromagnetics and the background of the refractive index and the method will be introduced, which are used to retrieve the intrinsic properties of the designed metamaterial. In chapter 3, most of the recent work that is related to high refractive index metamaterials done by researchers will be reviewed and the theoretical concept of the design of a novel dual band structure will be discussed. In chapter 4, design process and the simulation results will be shown and the optimization process of the structure will be discussed. In chapter 5, the retrieved parameters of the metamaterial such as the permittivity, permeability and the refractive index are discussed in order to show the advantage and the application of the proposed design.

Chapter

2. BACKGROUND: ELECTROMAGNETIC WAVE AND REFRACTIVE INDEX

2.1 Electromagnetic waves

Waves are disturbances that repeat itself over a distance in a medium, without altering the property of the medium. Waves in water are an example. Electromagnetic waves (Fig 2.1), like sunlight, carry electromagnetic energy and play an important role in our daily life including broadcasting, TV, microscope, imaging, lighting and cellphone, etc. The electromagnetic waves used in applications cover a broad range in frequency or what is known as the electromagnetic spectrum, which includes sunlight, radio wave and ultrahigh frequency waves like x ray and gamma rays.
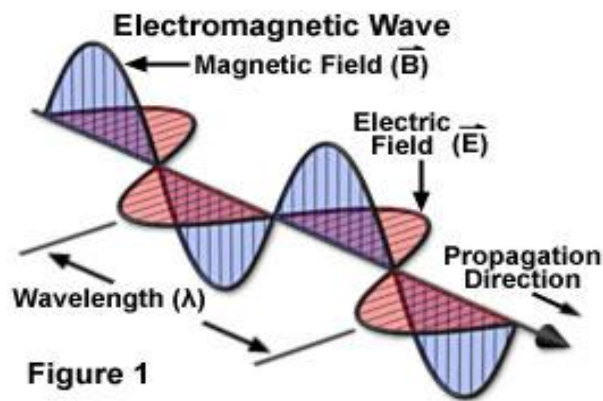
Fig. 2.1 Electromagnetic wave transportation [11]

Research on the propagation properties of the electromagnetic wave are done mostly in terms of its interaction with materials, specifically the effects of transmission, reflection, refraction of the electromagnetic wave and the intrinsic properties of the material. Most of the response of the material to an incident wave is

determined by the macroscopic electromagnetic properties of the material, also known as electric permittivity and magnetic permeability. Naturally existing materials usually have a positive dielectric permittivity and magnetic permeability value which enables the wave to behave in the way described through Snell's Law. In the past decade or so, scientists and researchers have broadened these enquiries to a much broader range of materials that are not available in nature, but are designed in a lab by humans and are termed as metamaterials.

Electromagnetic radiation, which is also called EM radiation or EMR, is a form of energy emitted and absorbed by charged particles, which behaves like a wave traveling through space as it is shown in Fig. 2.1. From the figure it can be seen that the propagating electromagnetic wave has both electric and magnetic field components, which oscillate perpendicular to each other in phase with a fixed intensity and are perpendicular to the propagation direction. In vacuum, the electromagnetic wave radiation propagates at the speed of light but at a variety of speeds in different medium due to the density and electric property of the carrier's material.

2.1.1 Electromagnetic spectrum

For clarity and convenience in application, one can classify EMR according to the frequency of oscillation. The classification of the EMR-electromagnetic spectrum consists of the entire frequency range including radio waves, microwaves, infrared radiation, visible light and ultraviolet radiation, X-rays and gamma rays. So the electromagnetic spectrum basically covers the whole range of all possible frequencies of electromagnetic radiation in the real world. The corresponding classification of the spectrum and the frequency range and energy of each band is provided in the figure

below in Fig. 2.2 as a reference. The general application of different frequency waves in everyday life are shown in Fig. 2.3.

CLASS	FREQUENCY	WAVELENGTH	ENERGY
Y	300 EHz	1 pm	1.24 MeV
HX	30 EHz	10 pm	124 keV
	3 EHz	100 pm	12.4 keV
SX	300 PHz	1 nm	1.24 keV
EUV	30 PHz	10 nm	124 eV
NUV	3 PHz	100 nm	12.4 eV
	300 THz	1 μm	1.24 eV
NIR	30 THz	10 μm	124 meV
MIR	3 THz	100 μm	12.4 meV
FIR	300 GHz	1 mm	1.24 meV
EHF	30 GHz	1 cm	124 μeV
SHF	3 GHz	1 dm	12.4 μeV
UHF	300 MHz	1 m	1.24 μeV
VHF	30 MHz	10 m	124 neV
HF	3 MHz	100 m	12.4 neV
MF	300 kHz	1 km	1.24 neV
LF	30 kHz	10 km	124 peV
VLF	3 kHz	100 km	12.4 peV
VF/ULF	300 Hz	1 Mm	1.24 peV
SLF	30 Hz	10 Mm	124 feV
ELF	3 Hz	100 Mm	12.4 feV

Fig. 2.2 Light spectrum [12]
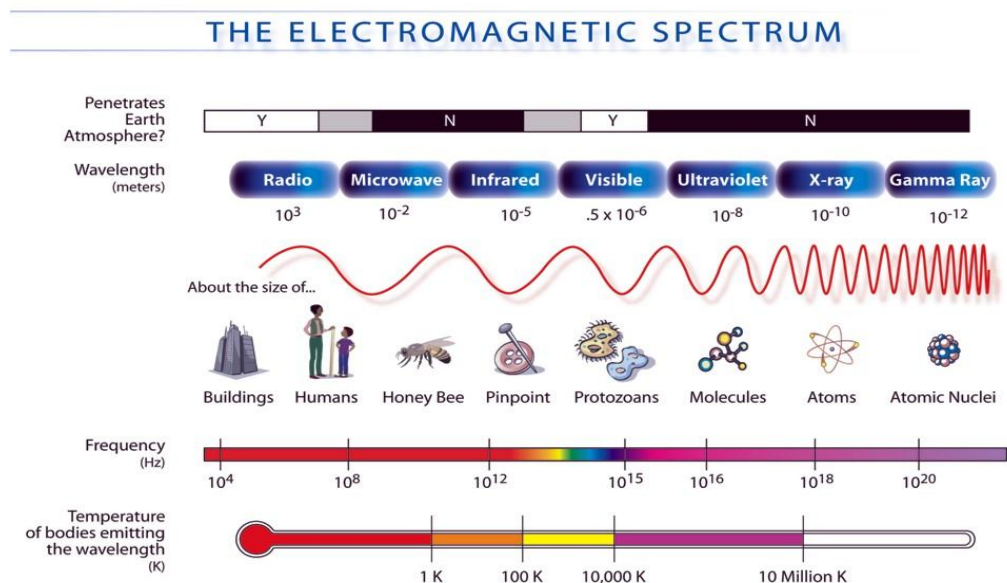
Fig. 2.3 Electromagnetic wave spectrum properties [13]

From the above figures, it is evident that electromagnetic spectrum extends from radio frequency to gamma radiation, covering wavelengths from thousands of kilometers to the size of an atom. Thus the electromagnetic spectrum is highly studied for spectroscopic purposes to characterize the properties and characteristics of all types of materials in the world.

2.1.2 Visible frequency and terahertz

The visible spectrum is being considered to be a special portion of the electromagnetic spectrum since it is visible to the human eye. A typical human eye will respond to wavelengths from about 390 nm to 750 nm which in terms of frequency is corresponding to a range of frequency from 400 to 790.

2.1.3 Introduction to terahertz

Terahertz (THz) radiation refers to electromagnetic waves with wavelengths that range from 100 μm infrared to 1.0 mm microwave as shown in Fig. 2.4. The THz band is the band where electromagnetic physics can be best described in terms of its wave-like characteristics in microwave frequency and its particle-like characteristics near infrared regime since its band position in the spectrum is adjacent to both frequency ranges.
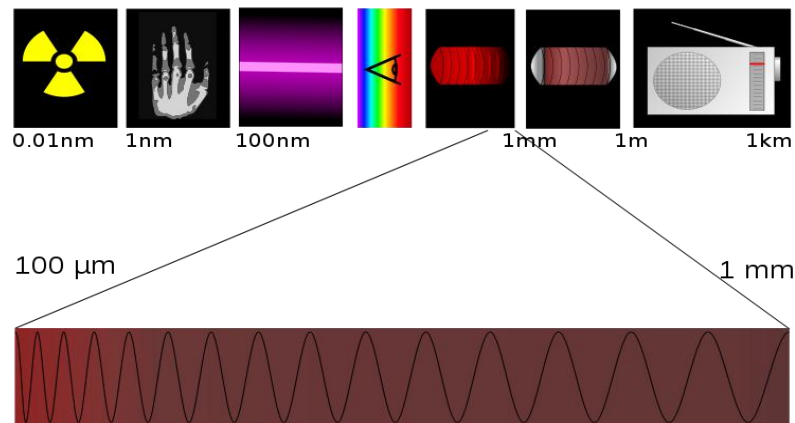
Fig. 2.4 Terahertz frequency range

With this dual characterization, terahertz radiation is classified as non-ionizing submillimeter microwave radiation. It has the capability to penetrate a wide variety of non-conducting materials such as clothing, paper, cardboard, wood, masonry, plastic ceramics and etc. It can also penetrate fog and clouds, but cannot penetrate metal or water. Due to this characterization, terahertz remains one of the most undeveloped frequency bands (which are so called the terahertz gap) because it has no reaction with many naturally existing materials which does not contain water. Also because of this property, there is an interest in investigating the interaction of terahertz frequency with the artificially made materials.

2.1.4 Terahertz safety

As stated earlier the terahertz region is between the radio frequency region and the optical frequency range which is generally associated with optical lasers. Both the IEEE RF safety standard [14] and the ANSI Laser safety standard [15] have limits into the terahertz region, but both safety limits are based on extrapolation. The terahertz frequency is expected to have thermal effects on tissues which contain water and it is predictable by conventional thermal models. However, research and experiments need to be carried out to verify the effects of terahertz wave and the safety limitation on human bodies.

2.1.5 Terahertz application

Interests in terahertz frequency radiation have existed for a long time. The terahertz frequency radiation has been considered to have a broad range of application in our everyday life. For example:

2.1.5.1 Medical imaging

Terahertz radiation has very little interactions with natural materials and thus has relatively low photon energy transferred to the tissue, resulting less damaging effects to the tissues of the material. Research shows that specific frequencies of terahertz radiation can penetrate several millimeters of tissue with very low reflection. Terahertz radiation can also detect differences in densities between water content and other tissues. Such advantages of terahertz frequency radiation could allow effective detection of cancer with a safer and less painful experience for the patient during the imaging process compared to those caused by x ray examination. Other frequencies of terahertz radiation can be used for 3D imaging of teeth in which it is considered more accurate than conventional x-ray imaging.

2.1.5.2 Security

Terahertz radiation can penetrate fabrics and plastics, which enables it to be used in surveillance, such as security screening at airports and other confidential area, to uncover concealed weapons or explosives without touching the human body. This is of particular interest because many materials have unique spectral "fingerprints" or characteristics in the terahertz range, thus making them easily to be detected by using terahertz radiation, specifically for security checking situation.

2.1.5.3 Other scientific applications

Another worth well application of terahertz radiation is that it enables art historians to see murals hidden beneath coats of plaster or paint in centuries-old buildings, without damaging the artwork or demolish the structure because it can penetrate materials. Besides, terahertz frequency radiation can be used in aircraft to satellite, or

satellite to satellite communication in very high altitude area where low frequency communication might lost signal and has bad quality.

2.2 Basics of refractive index
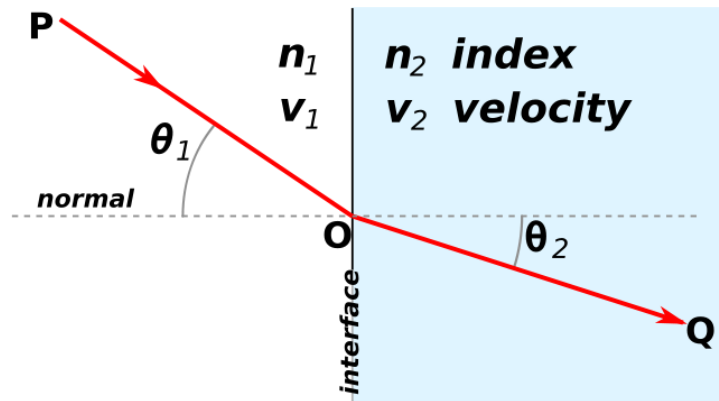
Fig. 2.5 Snell's Law [16]

In optics con the index of refraction of a material is a dimensionless number that describes how light or other radiation propagates throughout that medium. It is defined by Snell's law which relates how refraction index n has a relationship between the incident angle and the refraction angle by the formula $\sin \theta_1 \times n_1 = \sin \theta_2 \times n_2$, where θ_1 and θ_2 are the angles of incidence wave and the angles of the outgoing wave in regards to the normal of the interface of the material.

In another way, refractive index is defined as the factor by which the wavelength and the velocity of the propagating wave are reduced in the medium as it passes through with respect to their vacuum values. The speed of light in a medium is v = c/n, where c is the speed in vacuum while the wavelength in the medium is λ= /n. Difference in the refractive index causes the splitting of white light in prisms like the rainbows in the sky. The concept of refractive index is widely applied through the full electromagnetic spectrum, from radio wave frequencies to x ray frequencies.

2.2.1 Refractive index values

Most of the materials have refractive index values between 1 and 2 for visible light. For electromagnetic waves in the infrared frequency range, refractive indices can be somehow higher than those of the visible frequency. For example, Germanium is transparent in this region and has a refractive index of about 4, making it an important material for infrared optics. Just because most of the refractive index values in the natural material are limited 1 to 2, researches exploring high refractive index, low refractive index and negative index become more and more popular in recent years.

At the micro scale level, the phase velocity of an electromagnetic wave will be slowed down when transmitting in a material due to the disturbance of the charges of each atom induced by the applied electric field, which is proportional to the electric susceptibility of the medium. The same theory applies to magnetic field disturbance. As the electromagnetic fields oscillate in the wave, the charges in the material will also oscillate accordingly at the same frequency of the wave. Then the oscillating charges radiate their own electromagnetic wave that is at the same frequency with the applied wave but with a phase delay. So when there is an interaction with matter, the original wave plus the waves radiated by all the moving charges would be the final wave emitted outside of the material, which can be detected. This outgoing wave is usually a wave with the same frequency but shorter wavelength because of the deduction of the combined waves, which results in a slowed phase speed of the wave. Thus the relative phase speed of the original wave and the waves radiated by the moving charges will lead to several possible refractive index values, considering the different phase.

13

If the wave radiated by the disturbance is 90° out of phase with the original wave, the total wave will travel more slowly. This is the normal refraction of transparent materials like glass or water and corresponds to a refractive index value that is real and greater than 1. If the radiated wave by the disturbance is 180° out of phase with the original wave, the total light intensity will be reduced due to the total interfere with the original wave. This is light absorption in transparent materials and corresponds to an imaginary refractive index. If the radiated wave by the disturbance is 270° out of phase with the original wave, the total wave will travel more quickly. It corresponds to a refractive index less than 1.

For most normal materials in the real world at visible frequencies, the phase is always somewhere between 90° and 180°, corresponding to a combination of both refraction and absorption. In some cases where the response is sufficiently strong and out of phase, the result will be negative refractive index as discussed below.

2.2.2 Important properties related with refractive index

2.2.2.1 Snell's law

Snell's law is the basic law applied to most applications in electromagnetic waves and material interactions. In optics and physics, Snell's law is a formula used to describe the relationship between the angles of incidence and refraction waves, when referring to light or other waves passing through a boundary between two different isotropic media, such as water and glass. Snell's law states that the ratio of the sine of the angles of incidence and refraction is equivalent to the ratio of phase velocities in the two media, or equivalent to the opposite ratio of the indices of refraction, as descript in the formula $\frac{\sin \theta_1}{\sin \theta_2} = \frac{V_1}{V_2} = \frac{n_2}{n_1}$ where each θ is measured from the normal [16].

If there is no angle that satisfies Snell's law when waves traveling through a material as $\frac{n_1}{n_2}\sin\theta_1 > 1,$ the light cannot be transmitted and will have total internal reflection effects instead. This law is applicable to most of the materials in the real world and is also applicable to metamaterials, which will be discussed as the negative refractive index later.

2.2.2.2 Brewster's angle

Actually in most of waves interacting with a material, apart from the transmitted wave there is also reflected waves. According to Snell's Law, the reflection angle is always equal to the incidence angle of the wave, and the amount of reflected wave is determined by the reflectivity of the surface of the two materials. The reflectivity can be calculated from the refractive index value and the incidence angle with Fresnel equations, which is

$$R = \left| \frac{n_1 \times \cos\theta_1 - n_2 \times \cos\theta_2}{n_1 \times \cos\theta_1 + n_2 \times \cos\theta_2} \right|^2$$

Where n_1 is the refractive index of the material where the incident wave is and n_2 is the refractive index of the material where the outgoing wave is $\cos\theta_1$ is the angle of the incident wave with the normal of the interface while $\cos\theta_2$ is the angle of the refractive wave with the normal of the interface.

At a certain angle which is called Brewster's angle, waves with the electric field parallel to the plane of the incident wave will be totally transmitted and no wave is reflected back. Brewster's angle can be calculated from the two refractive indices of the interface as

$$\theta_B = \tan^{-1}\frac{n_2}{n_1}$$

2.2.2.3 Lenses

Metamaterials have been used in the design of lens, also called the perfect lens. The focal length of a lens is also related to the refractive index of the lens' material. The focal length of a thin lens in air is given by the Lensmaker's formula which is related to the refractive index of the lens:

$$\frac{1}{f} = (n-1)\left(\frac{1}{R_1} - \frac{1}{R_2}\right).$$

Where f is the focal length of the lens, n is the refractive index of the lens and R_1 is the radius of curvature of the lens on the focus point side while R_2 is the radius of curvature of the lens on the opposite side. Thus changes in the refractive indices of materials, as is the case with metamaterials, are likely to affect the lens properties.

2.2.2.4 Dielectric constant

The refractive index of a material can be calculated by the equation $n = \sqrt{\varepsilon_r \mu_r}$ where ε_r is the material's relative permittivity, and μ_r is the relative permeability of the material. For most naturally occurring materials, μ_r is very close to 1 at optical frequencies however, in the artificially made metamaterials, both the permittivity and the permeability could be tuned to a very high value or very low value, or even a negative value.

2.2.3 Negative refractive index

Negative index metamaterials (NIM), which is also called left-handed material (LHM) or double negative (DNG) metamaterials, are artificial made structures where the refractive index has a negative value in a specified frequency range. This characterization does not exist in any known natural occurring materials, and is only achievable with some specific engineered structures and materials, which is called metamaterials. In a broad theory, metamaterial refers to any artificial synthetic

16

materials with refractive properties that are different from the natural material, including ultrahigh refractive index, ultralow refractive index and negative refractive index.

Since Pendry's first introduction of metamaterials, many such negative refractive index metamaterials have been developed in order to manipulate electromagnetic radiation in new ways and obtain new properties that do not exist in the natural world. Researches and experiments have shown that with such metamaterial, optical and electromagnetic properties can be manipulated through tuning up the geometry of its unit cells. The unit cells are metallic structures that are ordered periodically in geometric arrangements embedded in the host material with dimensions that are much smaller that the wavelength of the electromagnetic wave applied to it. The response of the metamaterial to the electromagnetic wave is concluded to be much broader than that of the normal material both in strength and frequency range.

Theoretically, when a negative index of refraction occurs in a material, propagation of the electromagnetic wave will be reversed with an antiparallel phase velocity. The resolution below the diffraction limit becomes possible. This is known as sub-wavelength imaging. In contrast, conventional material lenses, like glasses, are usually curved and cannot achieve a resolution below the diffraction limit because of the reflection and diffraction of the transmitting wave. Furthermore, since negative index materials are customized composites with combinations of sub-wavelength structures, fabricating and manufacturing such materials have become a big challenge for scientists. .

2.2.4 High refractive index

For over decades, scientists have dedicated a large amount of time and effort to design artificial materials with properties that did not existent in natural materials. The refractive index is one of the properties in the nature that is hard to modify, yet changes could be useful. For example, consider the familiar scenes seen every day of a spoon in a glass of water which appear to be broken at the interface between air and water. The reason for this optical phenomenon is the change of refractive index between the two medium, which makes the route of light change. When light or wave passes from one material to another with different refractive indices, the direction of its propagation will change proportionally to the ratio of the indices of the two materials. Just because of this effect between different refractive indices, glass lenses can focus light and form images. Although this difference might be small, it can bend the light enough when it passing through a lens and focus the light on the other side of the material. As mentioned above, most of the refractive index of naturally occurring materials varies approximately from 1 and 2, which might limit how much the light can be bended for a specific application. Thus the thought come up to see if light could be bended further more with higher refractive index? The answer is yes, with the assistance of the metamaterials.

Actually a recent report from the Korean scientist gave a bright review on this. "I was curious about the limit of positive refractive index that is achievable with metamaterials," Min explained. "Researchers have been investigating negative refraction for the past years, but I believe that a high positive refractive index will also be useful for various applications, such as high-resolution imaging — preferably at the subwavelength scale — and very compact photonic devices." It is this motivation

that has pushed Min and colleagues to research on the metamaterial with a possible refractive index that is greater than 30 which is one order higher of the magnitude of the normal materials. Min and his colleagues' experiment appears to be the first to actually fabricated an artificially made material with ultra-high refractive index in the optical frequency range. The details of this work have been talked above in the literature review section already.

However, one drawback of this design is that it works well only in a single band of the terahertz frequency range. "Scaling to lower frequencies, such as to microwaves, will be quite easy as the tools for fabrication are readily available," Min adds. "However, it will be a more challenging task to scale down to the near-infrared or visible frequencies, as the fabrication of metamaterials in these regimes requires the most advanced nanofabrication technology."[17] With scientific advances in new nanofabrication techniques, it is clear that these metamaterials will emerge in different forms and designs, with scaled down frequencies to infrared with an extreme potential of light bending.

With the limitation and some drawbacks, this new discover greatly pushes the future development of the research on higher refraction index materials and thus triggers our interest on developing something beyond this invention with better performance in the index value and the effective operating frequency band..

2.3 Parameter retrieval

It is difficult to determine the intrinsic properties of materials from its look or size. The properties of the material need to be measured by applying electromagnetic waves and the properties can be measured from the results of the interaction with the material. For terahertz metamaterials, the mostly used measurement technique in

experiment is the THz-TDS method. The generated terahertz pulse pass through the target material sample and from the measured transmission and reflection on the receiving side, the electric permittivity and the magnetic permeability can be calculated. However, for simulation, there's no measurement of the material. S parameter retrieval method has become the essential methods in the recent years for the characterization of the metamaterial from the simulation results.

It is known that electromagnetic metamaterials are formed from either periodic or random arrays of scattering metallic elements and they should respond to the electromagnetic radiation as continuous materials. If an inhomogeneous material can be replaced by a continuous material, the scattering properties should be the same between the two materials. Then a procedure for the assignment of effective material parameters to an inhomogeneous structure consists of S parameters from a planar slab of the inhomogeneous material is compared to those scattered from a hypothetical continuous material. When the continuous material is characterized by a refractive index n and an impedance z, the relationship between the S parameters and the index and impedance can be found by the formulas listed below. The inversion of S parameters is the method that will lead to the refractive index and the impedance for the unknown materials [18]. The definition of the S parameters is shown in Fig. 2.7.
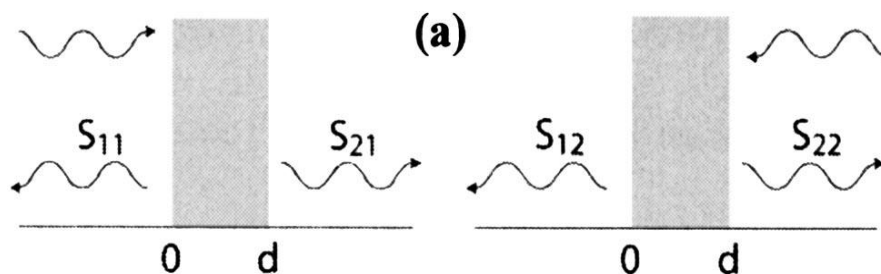

Fig. 2.6 S-parameter measurements on a homogeneous slab [18]

20

The approach for the inversion of the S parameters described here utilizes the transmission and reflection coefficients (S21 and S11) calculated from a wave normally incident on a finite slab of metamaterial. The scattering parameters are inverted to determine the index n and impedance z of the metamaterial. Though it is possible to completely specify the scattering parameters in terms of z and n, another set of analytic variables that can interpret the material directly are introduced in this presentation. These variables are the electric permittivity $\varepsilon=n/z$ and the magnetic permeability $\mu=n*z$ which is also related to n and z. Both n and z are frequency-dependent complex functions that satisfy certain requirements based on causality. For passive materials, Re (z) and Im (n) must be greater than zero.

Now the parameter retrieval process that is used in our design work will be discussed. The transmission coefficient is defined as t, which denotes the transmitted wave of the incident wave that is normally to the face of the slab of the metamaterial with a length d. The transmission coefficient is related to n and z by

$$t^{-1} = \left[\cos(nkd) - \frac{i}{2}\left(z + \frac{1}{z}\right)\sin(nkd)\right]e^{ikd}, \tag{1}$$

where $k=\frac{\omega}{c}$ is the wavenumber of the incident wave. For simplification of the calculation process and to improve the clarity of the subsequent formulas, the normalized transmission coefficient t'=exp(ikd)t is introduced. The reflection coefficient is also related to z and n by

$$\frac{r}{t\prime} = -\frac{1}{2}i\left(z - \frac{1}{z}\right)\sin(nkd) \tag{2}$$

Equations (1) and (2) can be inverted to find n and z as functions of t' and r. After the inversion operation it leads to the following expressions:

$$\cos(nkd) = \frac{1}{2t\prime}[1 - (r^2 - t\prime^2)] = \mathrm{Re}\left(\frac{1}{t\prime}\right) - \frac{1}{2|t\prime|^2}(A_1r + A_2t\prime) \tag{3}$$

21

and

$$z = \pm \sqrt{\frac{(1+r)^2 - t'^2}{(1-r)^2 - t'^2}} \qquad (4)$$

where $A_1 = r * t' + t' * r$ and $A_2 = 1 - |r|^2 - |t'|^2$ are both real value functions that go to zero if the material is lossless.

From the equation it can be seen that the expressions for n and z are complex functions with multiple branches because of the cosine function. The interpretation of such a cosine function can lead to ambiguities values in the final expressions of ε and μ. However by exploring additional information of the material these ambiguities can be cleared up. For example, if the material is passive, the requirement that Re(z)>0 fixes the choice of sign in Equation (4). If Im(n)>0 leads to an unambiguous result for Im(n):

$$\text{Im}(n) = \pm \text{Im} \left\{ \frac{\cos^{-1}\left(\frac{1}{2t'}[1 - (r^2 - t'^2)]\right)}{kd} \right\} \qquad (5)$$

When solving equation (5), whichever of the two roots yields a positive solution for Im(n) will be selected. However, Re(n) is more complicated by the branches of the arccosine function, or,

$$\text{Re}(n) = \pm \text{Re} \left\{ \frac{\cos^{-1}\left(\frac{1}{2t'}[1 - (r^2 - t'^2)]\right)}{kd} \right\} + \frac{2\pi m}{kd} \qquad (6)$$

where m is an integer. When d is large, these branches can be arbitrarily close to one another, making the selection of the correct branch difficult in the case of dispersive materials.

After determining n and z values, the electric permittivity and magnetic permeability values can be calculated by $\varepsilon = n/z$ and $\mu = n \times z$. When the equations programmed and applied in the MATLAB codes for calculation, the transmission "t"

22

is replaced by S21 and the reflection "r" is replaced by S11. The S parameters are results from the simulation by the commercial computational software MW Studio CST [19].

Chapter

3. LITERATURE REVIEW AND THEORETICAL BACKGROUND

Research in metamaterials and the discovery of their inherent characteristics are relatively new. The past decades or so has experienced a rapid progress in the design, development and application of metamaterials. This chapter provides a review of the work done, specifically in high refractive index metamaterials. The theory behind the specific characteristics of the designed materials is also included in the review. The title of this chapter is therefore based on this consideration.

The resonators embedded in dielectrics in the design of metamaterial have ranged from thin wires to split ring, and the resulting metamaterials have been applied in experiments from microwave to optical frequency. Researchers have discovered the properties of metamaterial such as negative refractive index and optical transformation. Perfect lens and cloaking devices have also been designed with the use of metamaterials. Metamaterials have been analyzed mostly in the microwave and optical frequencies; this research however is focused the THz regime.

Terahertz frequencies, which are in the region of the electromagnetic spectrum between 0.3 and 3 THz, are non-ionizing and it can penetrate a lot of materials except metals those materials that have water content. The property of terahertz frequency could bring a lot of valuable applications such as object detection and imaging. Since refractive index is an important factor that contributes to resolution of images, creating high refractive index materials could contribute to resolving resolution limitations imposed by the properties of current generation of lenses [20]. Metamaterial operated in terahertz frequency range are just the right candidate to utilize the features of terahertz frequency especially in the imaging process and

related areas. Designing a metamaterial with relatively high refractive index becomes more and more important in the resolution quality of the optical image. Development of high refractive index metamaterials have evolved in the past decade. The following paragraphs describe the history of high refractive index materials and the theoretical analysis of each structure, from the designer's perspective. The research presented in this works develops the concepts presented here, specifically high refractive index metamaterials. The research focus is on the development of a single metamaterial slab that exhibits high refractive at two distinct frequencies [21]. Most of the previous works, as discussed below, are based on high refractive index metamaterial at a single frequency.

Refractive Index with Embedded Metallic Film and Sub-wavelength Propagating Modes:

In 2005, J.T. Shen and his group demonstrated a dielectric slab with frequency independent effective refractive index [22]. The dielectric slab was made with a perfect metal film which was embedded with a periodic arrangement of cut-through slits. The experimental results showed that such a material can provide an effective refractive index which is entirely controlled by the geometry that can be manipulated to be arbitrarily high. Since the effective refractive index is usually considered to be the intrinsic property of a material, the author shows that the capability of manipulating the refractive index provides a potential way affecting the properties of the device for useful purposes.

To get the desired refractive index, the key is to demonstrate whether there exist sub-wavelength propagating modes in the metallic structures. A metal film was designed with one dimensional periodic cut through slits as shown in Fig. 3.1. The ambient environment surrounding the structure and in the slits are assumed to be

vacuum for generality. The author showed that in space between the slits, despite its width, there existing a propagating mode - TEM mode, with a generated electric field pointing in the x direction when the structure is exposed under a propagation mode in the y direction. It has been shown in the previous research that this existing mode ensures the perfect transmission of light through sub-wavelength slit arrays. For TM polarization, the slab will act as a high refractive index dielectric slab when the slits are much smaller than the wavelength of the propagating wave.
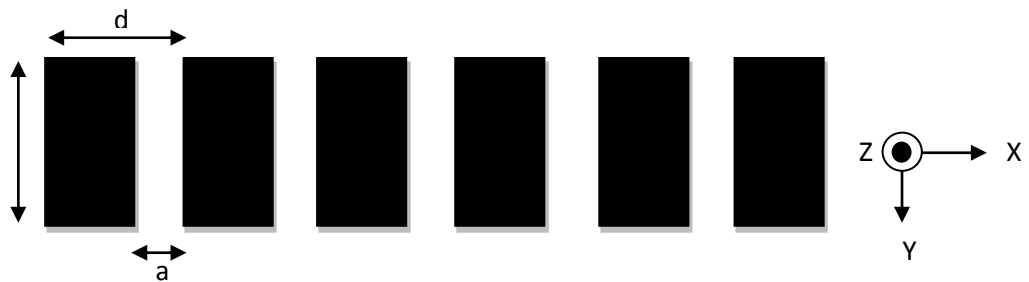

Fig. 3.1 Metal films with cut through slits [22]

Following a theoretically demonstration that metallic foam with periodic cut slits can behave as a dielectric slab with high refractive index, as suggested by Pinemov [23], J. T Shen conducted experiments to investigate metallic gratings with cut slits in dielectrics. The experiments demonstrated that a close similarity of the transmission and reflection coefficient of the fabricated metallic gratings with those of the dielectric slab. The transmission and reflection of both the metallic gratings and the dielectric slab using the Fresnel optical formulas was also demonstrated for comparison of the transmission and reflection values from the experimental result, as shown in Fig. 3.2.

To demonstrate the closeness of similarity of the metallic gratings and the dielectric slab, Shen used an MgO slab and the coincidence between the results of the experiment and that of the formula is of the same quality as the results of the metallic gratings and that of the formula. However, due to the phase shift, the equivalence between the dielectric slab and the metallic gratings is exact for the amplitudes but phase shift corrections were needed to get the exactly same results. To be concluded, by using the terahertz transmittance and reflectance spectroscopy a good agreement of the experimental result with the theoretical predictions can be demonstrated and thus the metallic gratings can be used for high refractive index materials. Equations $t = \frac{(1-r_0{}^2) \times t_1}{1-r_0{}^2 \times t_1{}^2}$ and $r = \frac{(1-t_1{}^2) \times r_0}{1-r_0{}^2 \times t_1{}^2}$ were used to calculate the value of the transmission power and reflection power of the sample materials. It is assumed that μ=1 in the experimental frequency range.
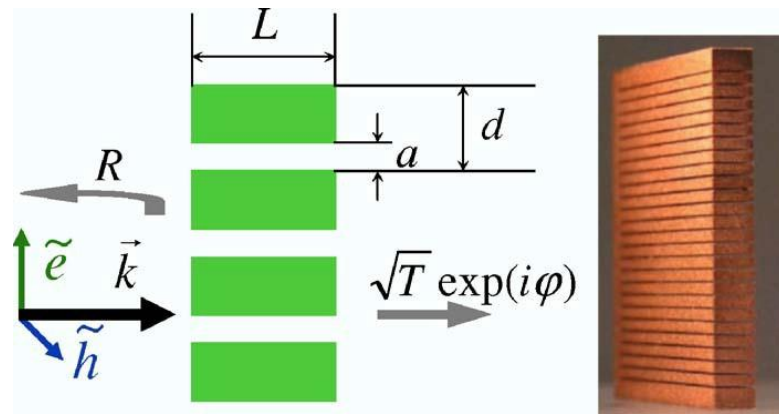

Fig. 3.2 Metallic gratings with cut slit [23]

Fig 3.3 and Fig. 3.4 shows the transmittance, reflectance and the phase shift of the metallic grating with L=2.01 mm in the experiment as well as the calculated data of the transmittance and reflectance using the above equations. The effective $L_{eff} = 0.372$ and n= 5.51+ (5.7+0.5i) $\times 10^{-4}$. The results demonstrate that the metal grating

structure can be represented by the equivalent effective dielectric slab with the effective thickness and the effective refractive index.
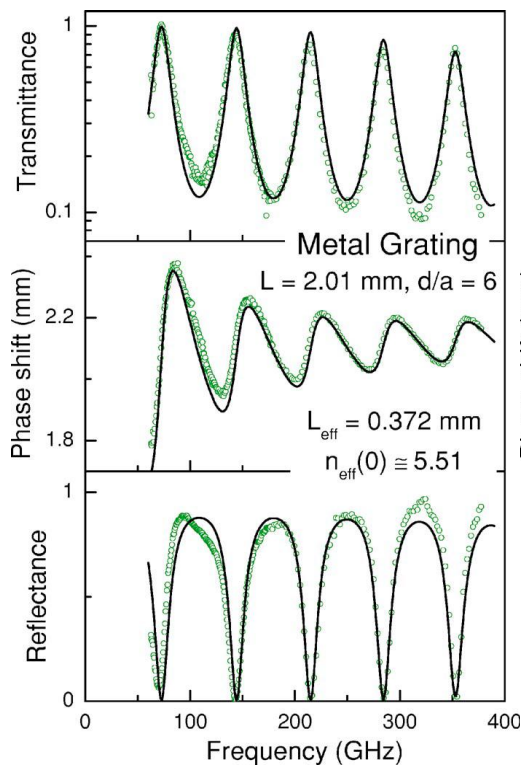

Fig. 3.3

Fig. 3.4

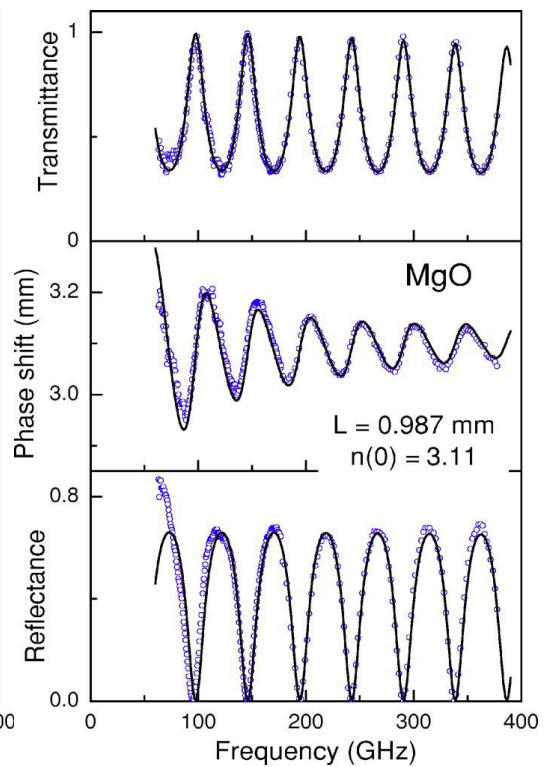Fig. 3.3 Transmittance phase shift and reflectance of the metallic grating for both experiment and calculation [23]

Fig. 3.4 Transmittance phase shift and reflectance of the dielectric slab for both experiment and calculation [23]

As a comparison, Shen also provided a plot of the transmittance, reflectance and phase shift of a plane parallel dielectric slab made of MgO with a thickness of $L_{MgO} = 0.987$ mm. In this case, the agreement between the experiment data from the metallic structure and the calculated values from the equation were very good as shown in Fig. 3.3 and Fig. 3.4.

The above work of high refractive index materials presented so far are based on metallic slab with periodic cut slits metamaterial that behave as an effective dielectric slab with the desired high refractive index. Most of these work intended to simplify

the system as two dimensionally freestanding lamellar gratings which support only the TEM modes of propagating waves.

Refractive Index with 2D and 3D Metal Slabs and Energy Momentum between Resonance Modes

In 2007, Y. Shin and his group looked into the difference of the energy momentum between the resonance modes in the 3D metal slab and that in the 2D metal slab [24]. To investigate the effect of the finite slit length to the refractive index of the material near the cutoff frequency of the slit waveguide, Shin's group demonstrated a 3D homogenization of a thick metal slab with 1D periodic cut slits as shown in Fig. 3.5.
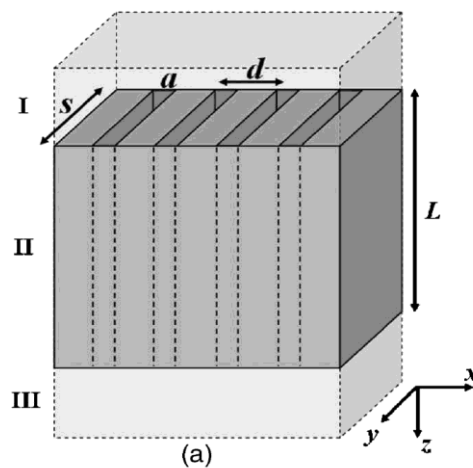

(a)

Fig. 3.5 Three-dimensional model of one-dimensionally arrayed subwavelength slits on thick metal [24]

By exploring the transverse field distribution of the even modes and the odd modes in the slits using the FDTD simulation method, it is concluded that the 3D metal slab with finite length sub-wavelength cut-slits has the frequency dependence. Their comparison between the theoretical and the numerical analysis showed that the varying refractive index induces a dense eigenmode population near the cutoff frequency, which leads to an energy level continuum in the slits. The results presented a guideline to engineers to produce the desired high refractive index metamaterial based on the dimensions of cut slits in a three dimensional structured metallic slab.

29

Refractive Index with Surface Plasmon Polaritons: *(high refractive index without electric or magnetic resonance)*

As stated above, J.T. Shen demonstrated a perfect metal film with periodic arranged cut slits to generate a frequency independent refractive index. The metal film with cut slits could be regarded as a dielectric slab and, by confining the electromagnetic modes in the highly subwavelength region with surface structures, the propagating transverse electromagnetic mode in the cut slits could be utilized in generating high refractive index in the microwave and infrared frequency range.

However, these results can only be achieved in this frequency range where the plasmonic effects of the metals can be mostly neglected. If applied in the optical frequency range, the plasmonic effects of the metals would generate additional subwavelength propagating modes which would adversely affect the high refractive index property.

In 2008, metamaterial structure utilizing the surface plasmon polaritons (SPPs) to generate high refractive index at visible frequency range was introduced [25]. Since most of the previous designs consisted of metallic plates and wires that operated near the resonant frequency, H. Shi and his group believe that the surface plasmon polaritons excited in the metallic surface at the visible frequency range must have considerable effect on the artificially made metamaterial's property. Based on this assumption, a plasmonics metamaterial with excitation of SPPs was proposed. The designated material's resonance property was not only determined by the structure geometry but also depended on the dielectric function of the metal used, since the excited SPPs depend on the nature of the surface of the metallic structure. Researches were done on the interaction between the surface plasmon modes and its effect on the generation of the high refractive index in the subwavelength metallic channel. The

30

result suggested that one of the biggest benefits of the designed structure is that it can generate required high refractive index without any electric or magnetic resonance along the geometry and the loss of material is reduced significantly. The proposed structure is shown in Fig. 3.6 which is similar to that of the design by Y. Shin. High index of reflection in the subwavelength channel between the metallic slabs was generated at the visible frequency by the interaction between the surface plasmon modes of the adjacent surface of the metallic slab.
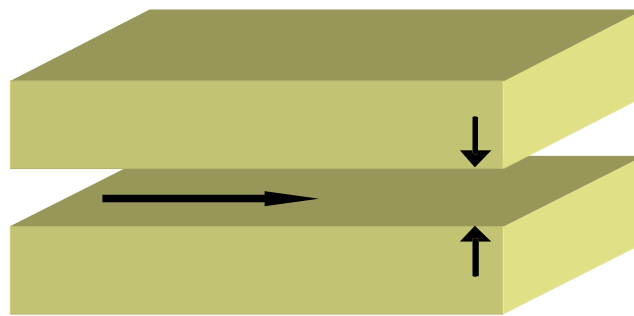
Fig. 3.6 Metallic slit unit [25]

So far, the design of the high refractive index metamaterials has gone from the microwave frequency range to the optical frequency range. The method to achieve this goal is not only limited to manipulating the geometry of the structure but extended to controlling the interaction of the surface plasmon modes of the metallic structure.

Refractive Index due to Plasmonic Resonance:

With the process of understanding the mechanism of plasmonic resonance and the fabrication technology's advancement, a new design utilizing the plasmonic effect was introduced by X. Wei and his team in 2010 [26]. The new design was easier to fabricate and has better performance at optical frequency range. Here, a stack of cut wires were introduced to demonstrate the plasmonic effects in the metals and only the

31

electric resonance of the cut wires induced by the surface plasmons on the metal structures was emphasized. The magnetic response was not taken into consideration in this work so far till now. The author aimed on the study of the dependence of the effective refractive index on different design parameters of the structure and the optical properties of the nanometer structure by experiment.
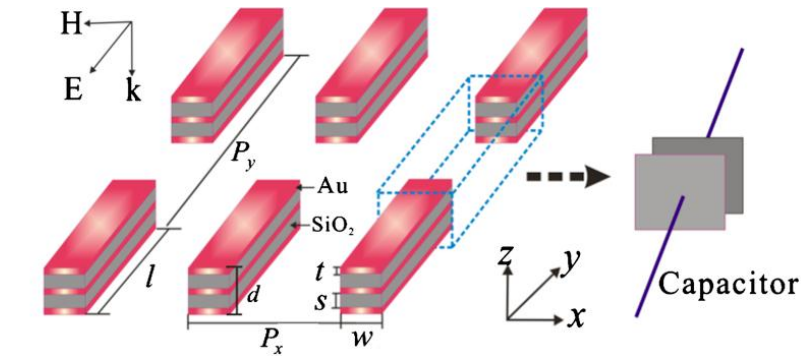

Fig. 3.7 Three layers stacked metallic cut wires [26]

As shown in the Fig. 3.7, triple Au cut wires were designed periodically in a planar shape. An electromagnetic field with time varying electric field in the y direction was applied to the cut wires and surface plasmons were excited because of the interaction between the incident photons from the electromagnetic wave and the free electrons in the metal. A large amount of electric charges were induced and accumulated on the edge of the cut wires resulted in energy stored in the gaps of the cut wires, thus enabling the gaps to be effective capacitors. This way, the whole cut wires were considered to be electric resonators with the capacitive effect between the gaps which leading to the high value of the permittivity.

The simulation result and the measurement result showed good agreement. The author also studied the effects of the geometry of the cut wires and found that the longer the cut wires, the higher the index of refraction since the gap between the wires

became smaller while making the wires longer. Ultimately, X. Wei and his group demonstrated a successfully designed cut wire metamaterial that could be used in the optical frequency range with high refractive index. The result showed that the index of refraction depends only on the geometry of the structure.

However, in the design by X. Wei, the diamagnetic effects were not taken into consideration, and the magnetic anti-resonance in the structure affects the refractive index. The relative permittivity is determined by the charges on the surface normal to the electric field and the relative permeability is determined mainly by the magnetic dipole moment and the area that is surrounded by the current loops on the surface that is parallel to the magnetic field. Thus to increase the refractive index of a metamaterial is to enlarge the electric response and reduce its magnetic dipole moment. This magnetic anti-resonance problem was solved by J. Shin which eliminated the diamagnetic effects [27], which showed high relative permittivity as well as high permeability. J. Shin proposed a method for reducing the surface of the structure of a metallic cube by cutting slit on it to decrease the diamagnetic effect of the structure. In this method, a metallic cube with six metallic plates connected by three metal wires in the center was invented. Then the plates were cut into slits to reduce the area surrounded by the current loop on the surface of the plate. Further, the structure was reduced to a bell shape as described in Fig. 3.8 to further suppress the diamagnetic effect and maintain the electric response in regards to the well-known fringe-field effect by [28, 29]. The FDTD simulation results showed improvement in the permeability value on the structure compared to that of the cube, with a relative permeability of 0.966 which is really close to 1 and a relative permittivity of 18.3 and a refractive index of 4.2. The loss of the metamaterial was also taken into

consideration in this work and it showed low loss for the designed material so the important electromagnetic effects can be observed more effectively.
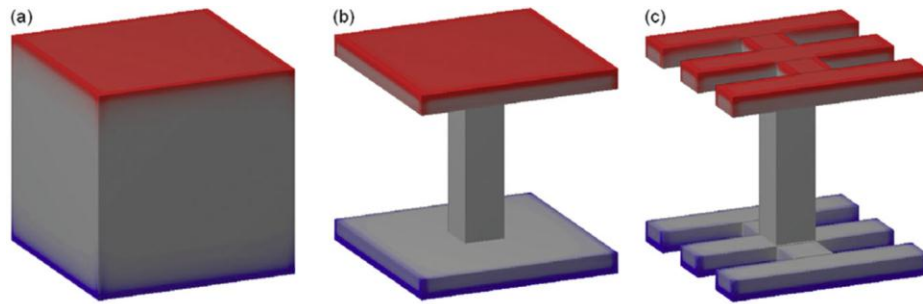

Fig. 3.8 Electric field on the tailored structure [27]

It was concluded that an enhancement of the refractive index is achievable with the mechanisms introduced and the only factor that affected the result was the shape and geometry of the unit cell. This work provided a new way and efficient way to design a novel metamaterial with high refractive index with low diamagnetic effects.

Inspired by J. Shin's design, Dr. M. Choi and his research group proposed and developed the "I" shape structure with ultra-high refractive index, on a free-standing flexible substrate [30]. The metamaterial consisted of strongly coupled "I" shape unit cells which were made with gold and embedded in a substrate made of polyimide. High effective permittivity was possible by increasing the capacitive coupling of the structure as well as decreasing the diamagnetic response with a specifically designed ultra-thin "I" structure. The fabricated structure is shown in Fig. 3.9. With a thin metallic structure, the area surrounded by the current loop parallel to the magnetic field is minimized such that the magnetic dipole becomes very small. With advanced technology of nano scale fabrication, the structure was easy to fabricate. Measurement of the fabricated structure showed a relative ultra-high refractive index with a low loss of the power transmitted, which was also very close to the simulation results. Since

the structure is fabricated with the metallic structure embedded in a polyimide substrate, the metamaterial showed greater flexibility. Dr. M. Choi also demonstrated the performance of a multilayer structure which showed broader band of resonant frequencies. He proposed that for the improvement of the structure, either the gap between the metallic structures could be reduced or the layer of the structure could be increased to achieve even higher refractive index. Since the operating frequency of the metamaterial structure depends mainly on manipulating the geometry of the structure, the application and design of metamaterials can be extended to both lower frequency ranges such as microwave frequency and higher frequency range such as infrared and visible frequencies.
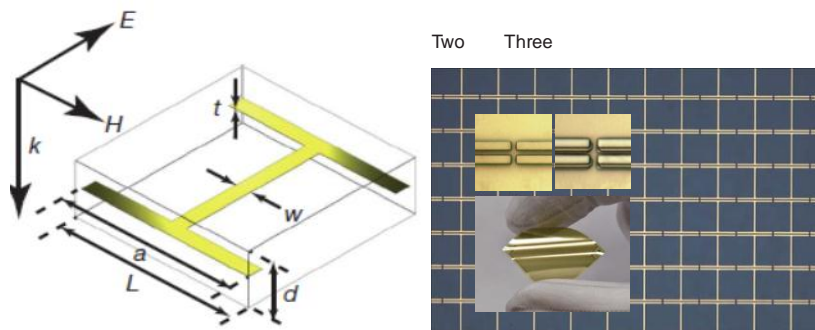
Fig. 3.9 Unit cell structure of the high-index metamaterial made of a thin 'I' shaped metallic patch symmetrically embedded in a dielectric material [30]

By pointing out multiple applications of the high refractive index metamaterial in the real world, Dr. M. Choi also mentioned that this design could be used as the ideal candidate for the sub wavelength scale functional devices such as small-footprint cloaking devices, wide-angle metamaterial lensed, compact cavity resonators and broadband slow light devices with its advantage of rapid phase advance.

So far a couple of different designs with high refractive index from microwave frequency to visible frequency range have been reviewed. Since more and more focus has been put on the terahertz frequency range because of its emerging applications and advantages, high refractive index metamaterials in terahertz frequency become goal of the design that is going to be presented later. However, within the design of the terahertz high refractive index metamaterials, all the concern is the performance of the material in a single frequency band. It's intuitive to come up with the idea about a dual frequency band or a multiband material. Some research work has been done during the past few years on the structures with two resonant frequencies within terahertz frequency. These research works have broadened the scope of designing a metamaterial with high refractive index at dual bands or more bands within the operating frequency range. Before going into the design of the dual band high refractive index metamaterial, brief overview of the dual resonant frequency structures in terahertz frequency range will be provided and the a mechanism of designing the dual high refractive index metamaterials will be illustrated.

In 2008, Y. Yuan and his colleagues demonstrated an ELC resonator based metamaterial structure with two distinct resonant frequencies in the terahertz range, which is motivated by the advantages of ELC resonators and the application of terahertz spectrum of electromagnetic waves. Since the ELC resonator does not require connection between unit cells and can be manipulated with the geometry parameters to realize the desired electric response in the desired operating frequency, it becomes really desirable right after it has been invented. Besides, the flexibility of the ELC resonators enables the fabrication of a planar metamaterial to be easy and flexible.

Attracted by the potential use and application of the multi-resonant frequency metamaterials, a dual band planar electric metamaterial was designed and fabricated by Y. Yuan etc. using the ELC resonators [31]. The designed structure was composed of two single resonant particles connected together with the first resonance near 1 THz and the second resonance near 1.5 THz as shown in Fig. 3.10. The upper particle is larger than the lower particle. The smaller the size of the particle, the higher resonant frequency it has in the operating frequency.
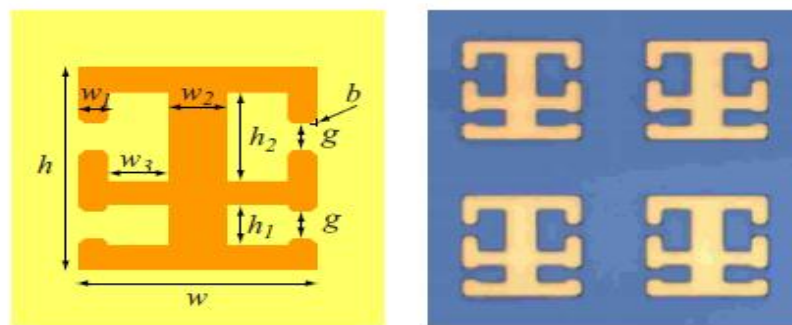
Fig. 3.10 Designed unit cell and Photomicrograph of the fabricated sample [31]

Different combinations of the particles were compared for different resonant frequencies in Fig.3.11. The simulation result showed that the upper particle contributes to the lower resonant frequency and the lower particle contributes to the higher resonant frequency, while the combined structure shows a good result of dual band resonant frequency in the desired frequency range.
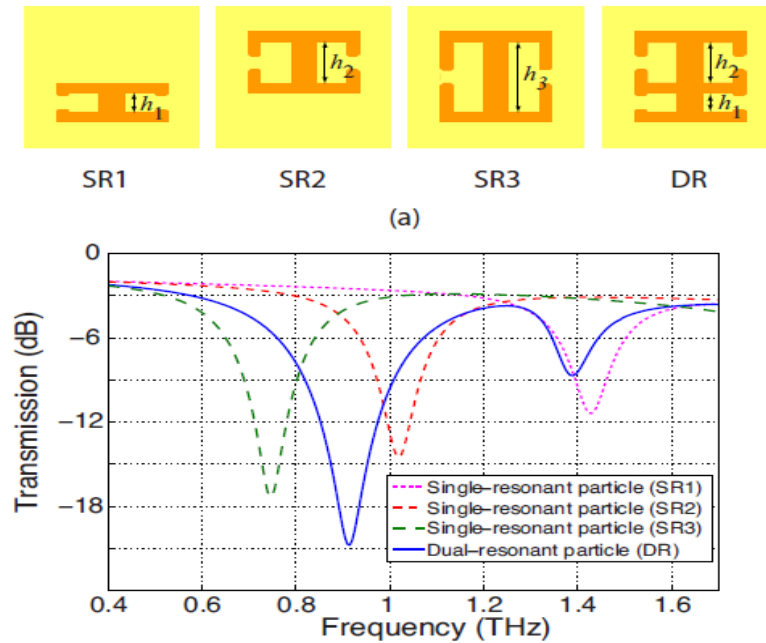
Fig. 3.11 Single-resonant particles SR1, SR2, SR3, and DR with corresponding calculated

transmission plot [31]

The experimental as well as the simulation results were compared by author. Yuan and it showed a good coherent in the operating frequency, with two resonances in near 1 THz and 1.5 THz.

Another work which was done by D. R. Smith's group also showed a good dual band resonant structure in terahertz regime in 2008 [32]. By the time when the paper was published, all the reported works done by D. R. Smith's group have exhibited single band electric or magnetic response. Thus, the dual band planar electric metamaterial with two distinct resonant frequencies was proposed as well as a method to define the effective thickness of the metamaterial layer. In addition, to obtain a good agreement between the simulation and measurement result, Dr. Smith suggested to separate the metamaterial into two layers, one is the effective metamaterial layer while the other one is the substrate layer with a proper model of the loss of the substrate. The proposed structure and simulation results are shown in Fig. 3.12 and

Fig. 3.13 where the two resonant frequencies are clearly seen in the plot of the transmission.
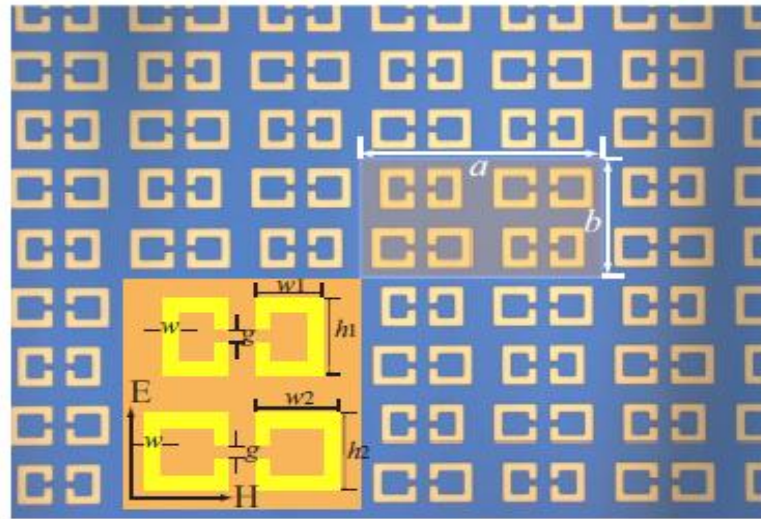
Fig. 3.12 Photomicrograph of the fabricated dual symmetrical SRR sample [32]
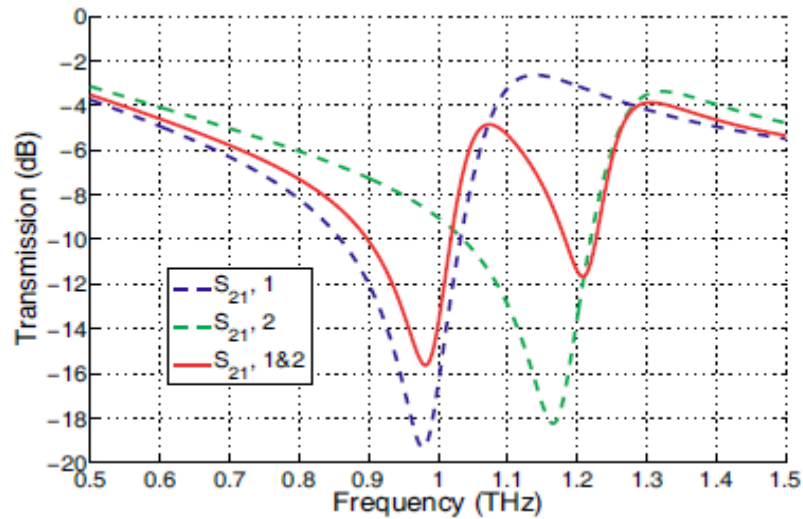
Fig. 3.13 Simulated transmissions (in dB) of the dual-band electric metamaterial (solid line), and of the individual symmetrical SRRs (dashed lines) [32]

With the suggested method, a dual band electric resonator was fabricated. The planar structure composed symmetrical SRRs opposing with each other to eliminate the magneto electric coupling effect. The metamaterial contains two sizes of the

symmetric SRRs to have two distinct resonant frequencies excited in the frequency range. As seen in the figure, the structure might have purely electric resonance if the electric field is orthogonal to the gaps in the structure with no magnetic couplings since the magnetic field is parallel to the SRR plane. In this case, it is able to control the electric resonance of the SRR purely and separately. The metallic SRR structure is fabricated on the GaAs substrate for its good isolating property and wave performance under the electromagnetic waves.

During the research, the effective thickness of the metamaterial was also decided by using the convergence of the resonant frequency for different thicknesses. To maintain the maximum of the capacitive resonance for the gaps and the maximum of the extension of the wave in the substrate, a 10 um thick substrate was made when the resonant frequency converged.

The simulation is based on a three layer system with one SRR layer, one substrate layer and one air layer to obtain the s parameters of the metamaterial. The simulation result shows two distinct resonances in the transmission plot. However, since the structure has three layers, the reflection of the wave is different considering the incident wave direction either towards the SRRs or the substrate. In the conclusion, the simulation and the measurement of the structure matches very good and a dual band structure was successfully made. However, the problem of the asymmetric of the structure layers may cause complication when measuring or simulating the structure with incident waves. So the proposed structure will be made symmetric for both way of the incident wave and there's no difference for incident wave from different directions.

Another drawback of the mentioned ELC structure is that it does not show sufficient intrinsic parameters about the material. The behavior of the material with electromagnetic waves needs further study. Particularly, more attention needs to be paid on the refractive index of the designed structure as an improvement of the previous single band structure and as to fill up the terahertz gap application.

Based on the work of the Y. Yuan's group, the concept to integrate two structures together to get the combined resonant frequency from the two structures separately is adopted in this research. The novel I shape structure as the main resonant structure is used as well as a set of cut wires in the "I" shape structure are used as a second resonance source. The proposed structure can be treated as a brand new structure with multiple applications and advantages. The design process of the new structure will be discussed and the results will be demonstrated in the later chapters.

Chapter

4. SIMULATION SET UP AND RESULTS

This chapter will discuss the design process, and the structure schematic and analysis of the new metamaterial with high refractive index at dual band frequencies. The design idea originates comes from a previous work [30], where a number of modifications are introduced in order to generate two high refractive index values at two frequencies for the structure. Also, in the parameter optimization process, (presented in the next chapter, different geometry parameters of the structures are compared and the best geometry for the design frequency are given for both the original and the new designed structure.

4.1 Simulation set up

In this section, simulation and software set up procedure will be discussed to demonstrate how the structure is designed in the modeling process.

4.1.1 Unit set up.

For minimizing memory space and fast conversion, it is important to choose the right simulation units. The following step is to set up the unit for the designed structure. Since THz frequency is used, the dimensions are in micron and the simulation time is set to picosecond correspond to the simulation frequency. The voltage and current remains the default value.
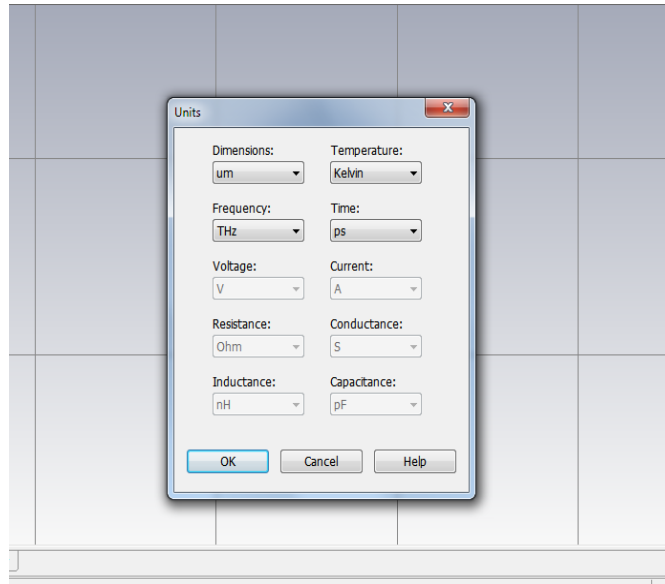
Fig. 4.1 Unit set up screen

4.1.2 Background material

The background material needs to be set up as normal. The other electrical and thermal parameters remain the default. The surrounding area are set to be further in the z direction considering this is the direction of the wave propagation and with this setup, the simulation results become smoother than that without the additional area in the z direction.

4.1.3 Frequency

The operating frequency range is set up from 0 to 3 THz since the main concern is the performance of the metamaterial in the lower terahertz range since this frequency band in the lower spectrum is essentially important in the applications of detection, security and in the biology and chemical areas. Fig 4.3 shows the window in MW Studio CST for frequency set up.
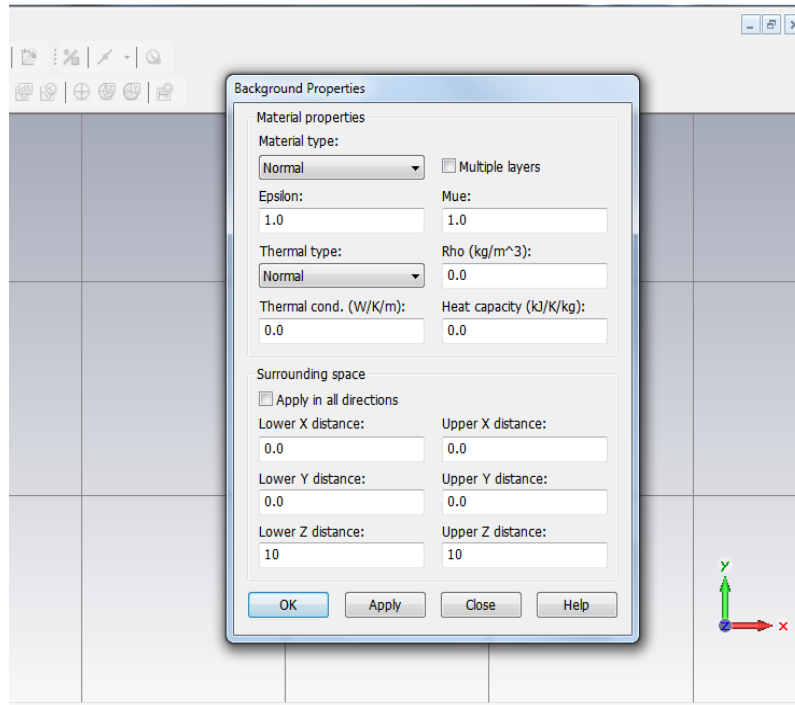
Fig. 4.2 Background set up window
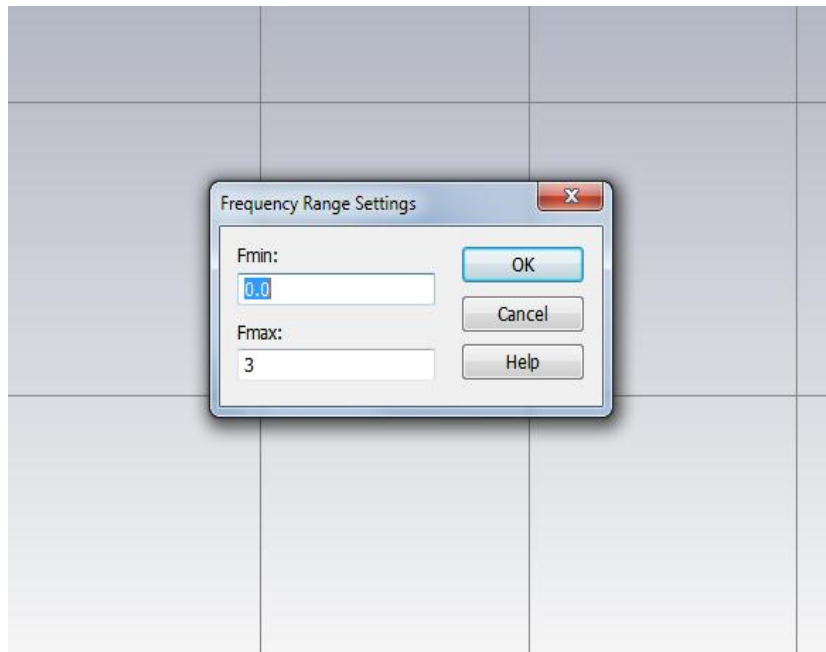
Fig. 4.3 Operating frequency set up

4.1.4 Boundary conditions

Fig.4.4 shows the boundary conditions setup of the designed environment. As shown in the figure, the x direction is the H field y direction is the E field and the z direction of propagation of the incident wave.
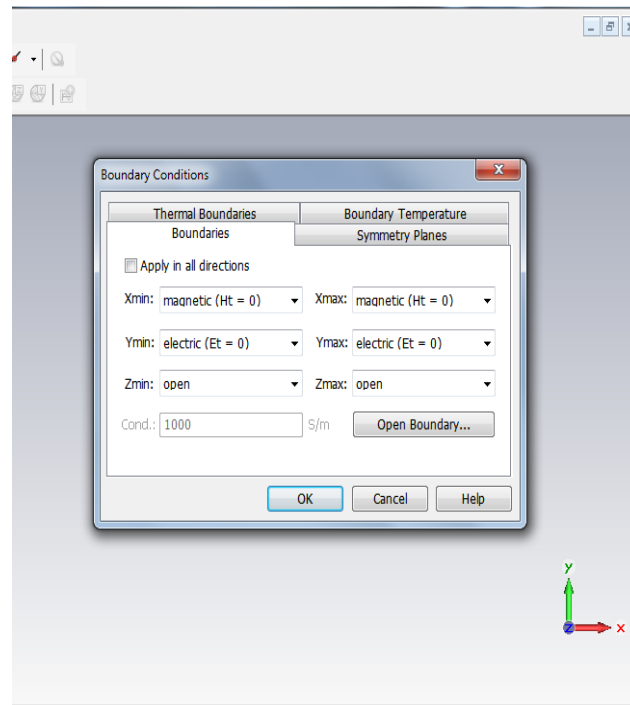
Fig. 4.4 Boundary conditions set up
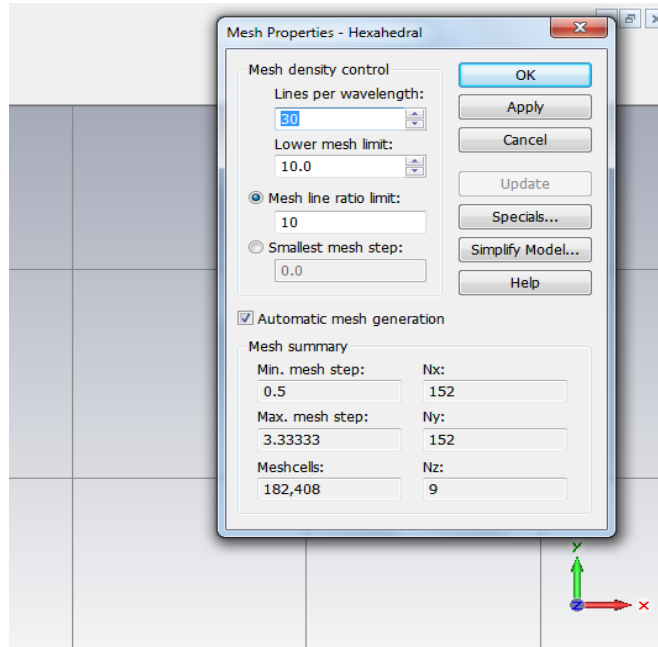
Fig. 4.5 Mesh cell set up

Finally the mesh property is set up to get accurate simulation results but with the fast simulation time possible.

4.2 Structure design

Following background conditions set up, the design of the structure is the next step in the simulation exercise. Here the original structure with the "I" shape is designed first. Then two sets of cut wires on the sides of the center bar connecting with the "I" shape structure are added. All transmission and reflection result are discussed in chapter 5. Every single structure of the design is listed step by step in the figures from Fig. 4.6 to Fig. 4.13. The configuration of the dimensions for each part is included in the plot on the right top corner. The material for the yellow region (metallic structure) is made of gold and the structure surrounding it is the foam made of polyimide.

The dimensions shown here is a sample with a random value for each part. The figure in the following shows the dimensions and the values are listed in table I.
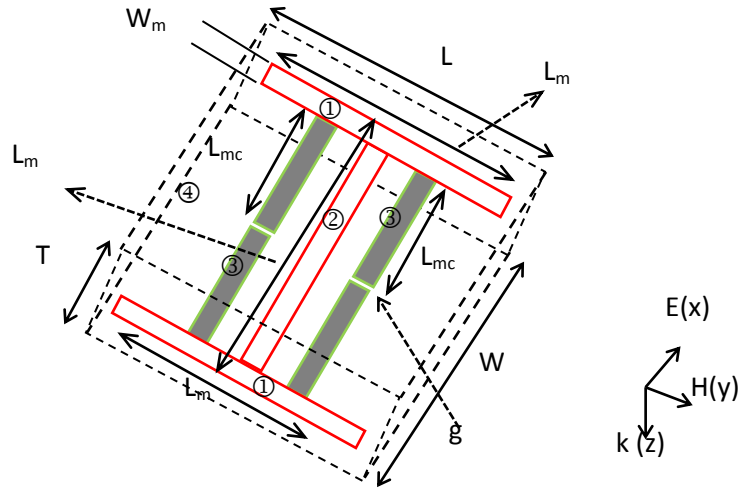
Fig. 4.6 Schematic plot of the a unit cell the proposed structure

TABLE I
DIMENSIONS AND COMPONENTS OF THE
DESIGNED STRUCTURE

Location		Length	Thickness
		Width	
Top and bottom bar, Au	①	L_m=49um	0.1 um
		W_m=1.5um	
Center bar, Au	②	$L_m-2\times W_m$=46um	0.1 um
		W_m=1.5um	
Cut wires, Au	③	g=L-W; L_{mc}=(46-g)/2	0.1 um
		W_m=1.5um	
Substrate, Polyimide	④	L=50um	5 um
		W=49um	
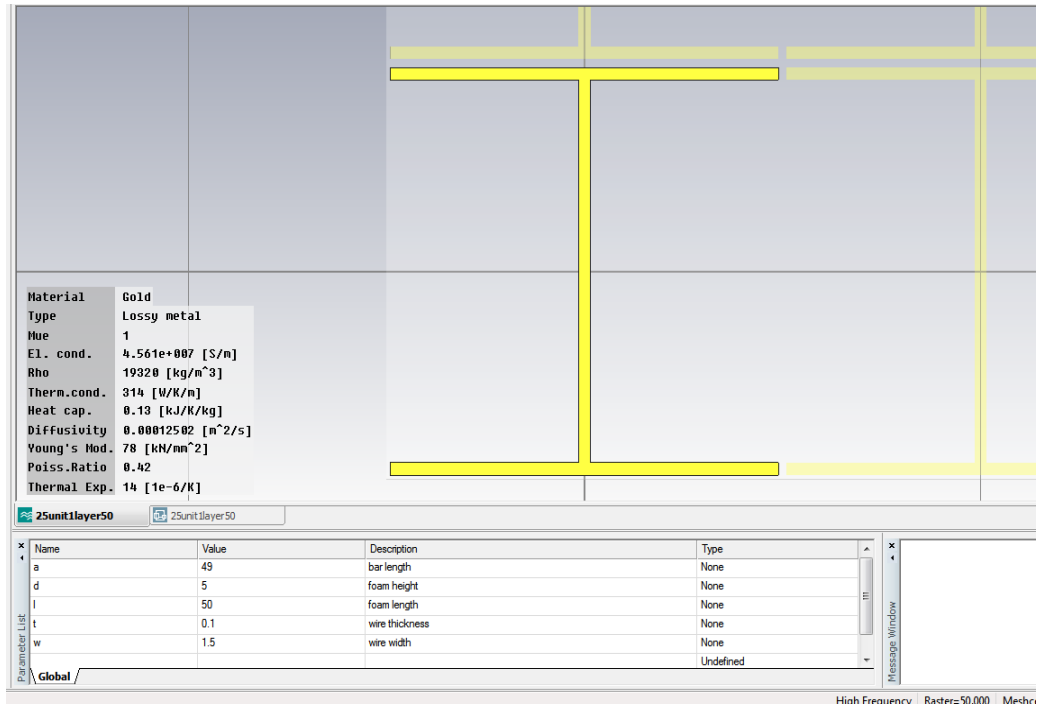
Fig. 4.7 The original "I" shape structure
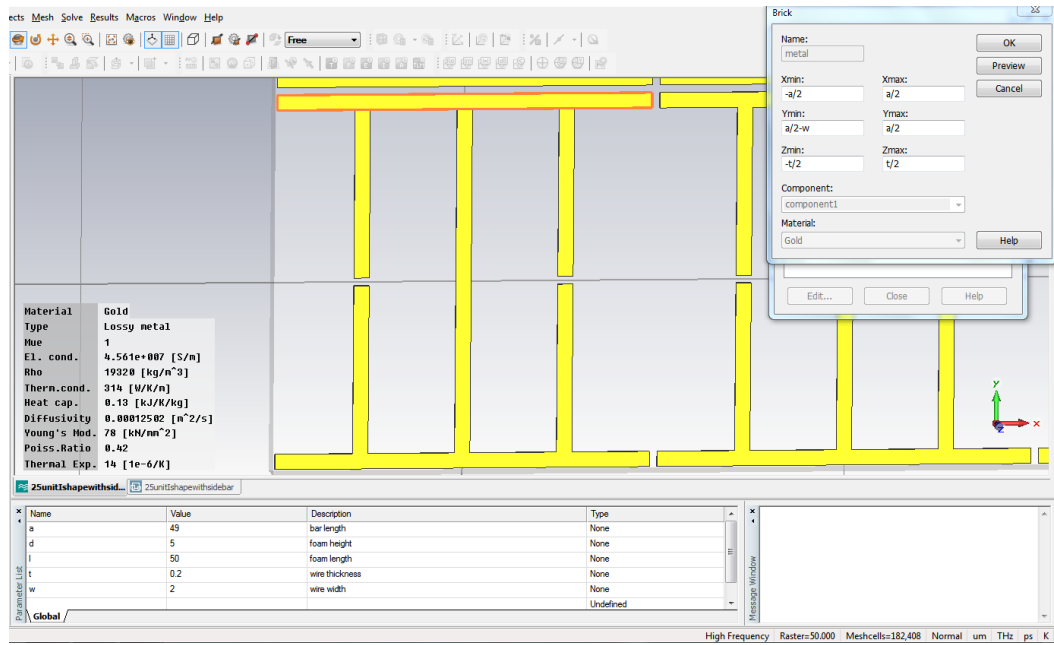
Fig. 4.8 Define the parameters of the proposed new dual band structure
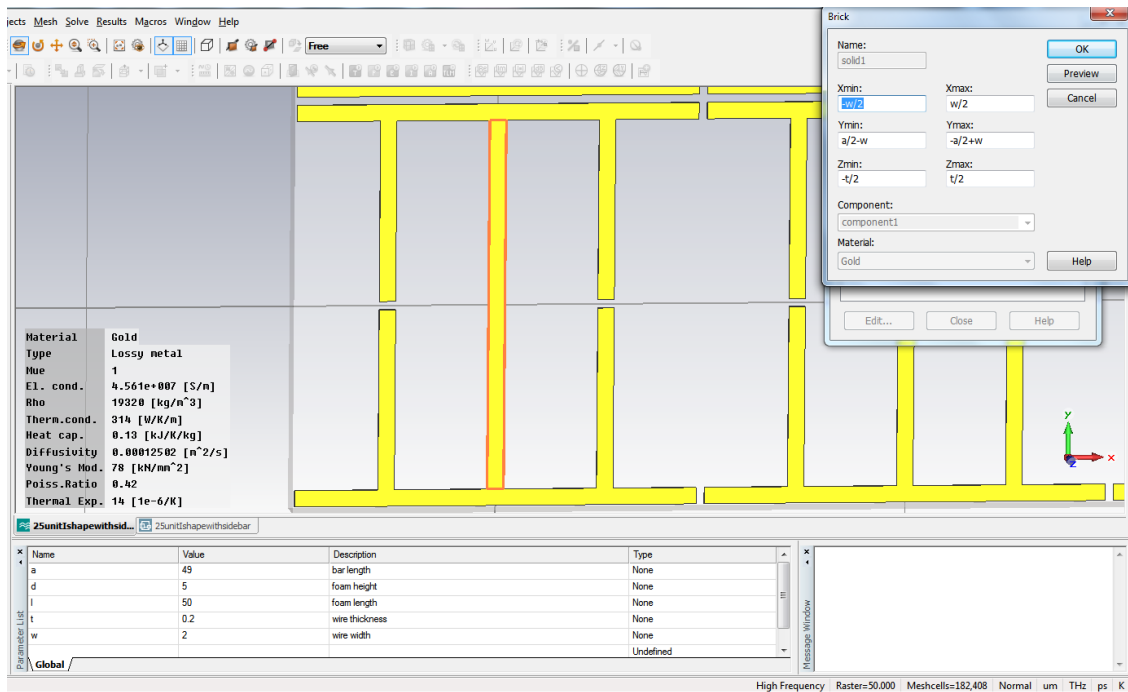
Fig. 4.9 Define the center bar dimension
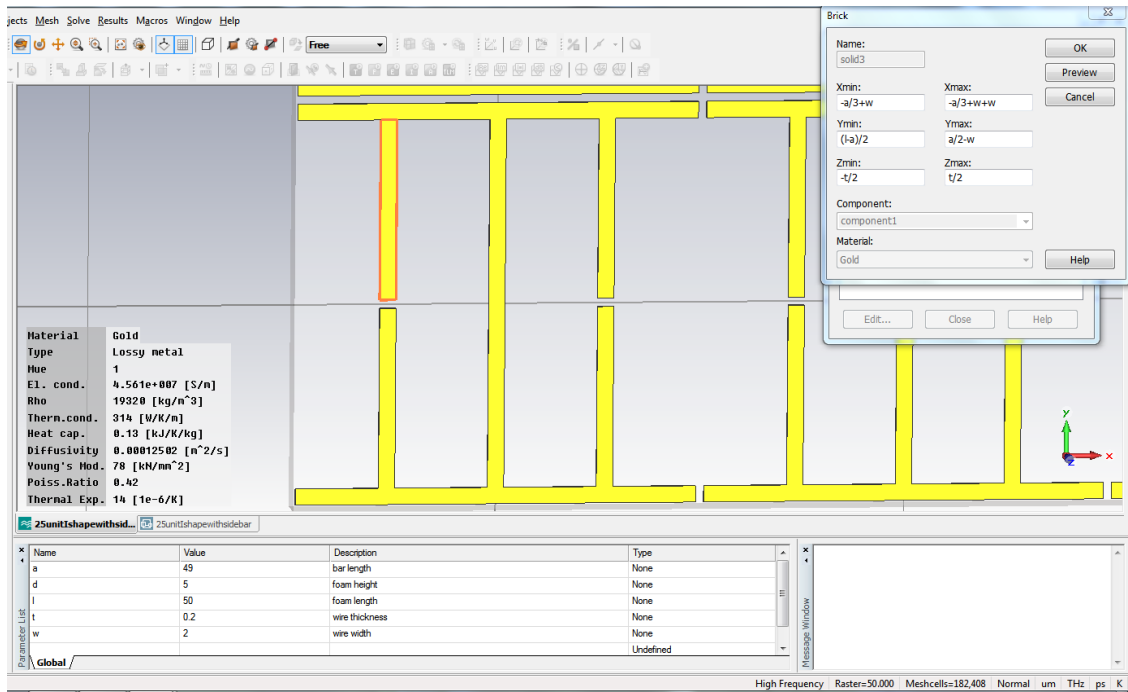
Fig. 4.10 Cut wires dimension set up
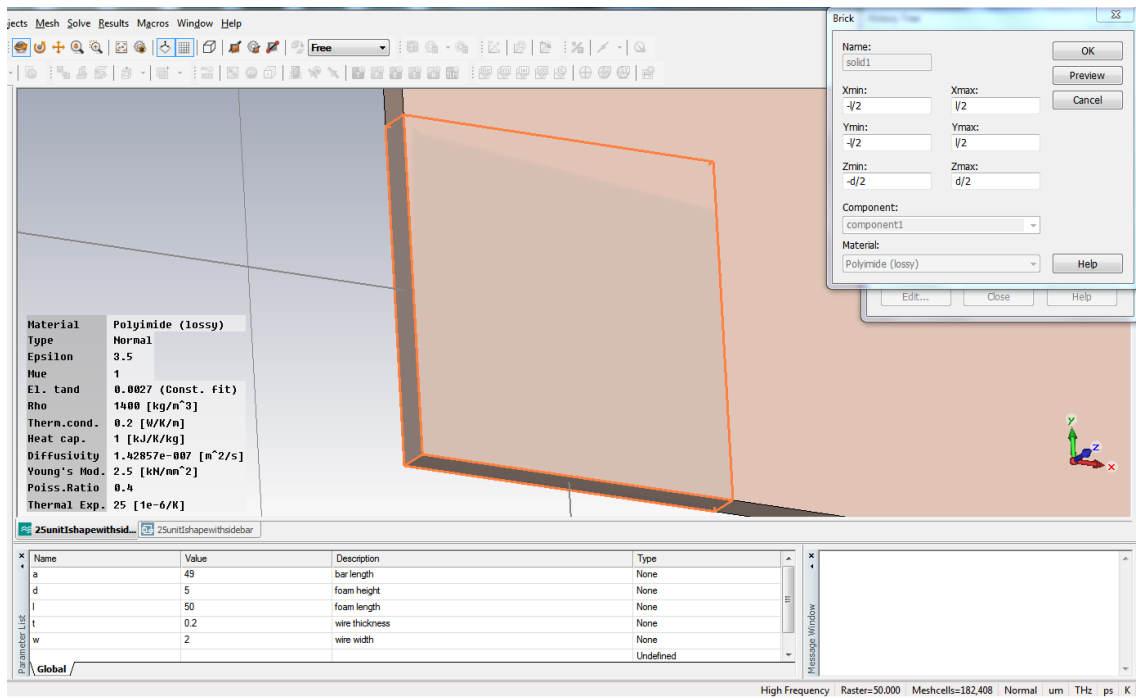
Fig. 4.11 The substrate of the designed metamaterial
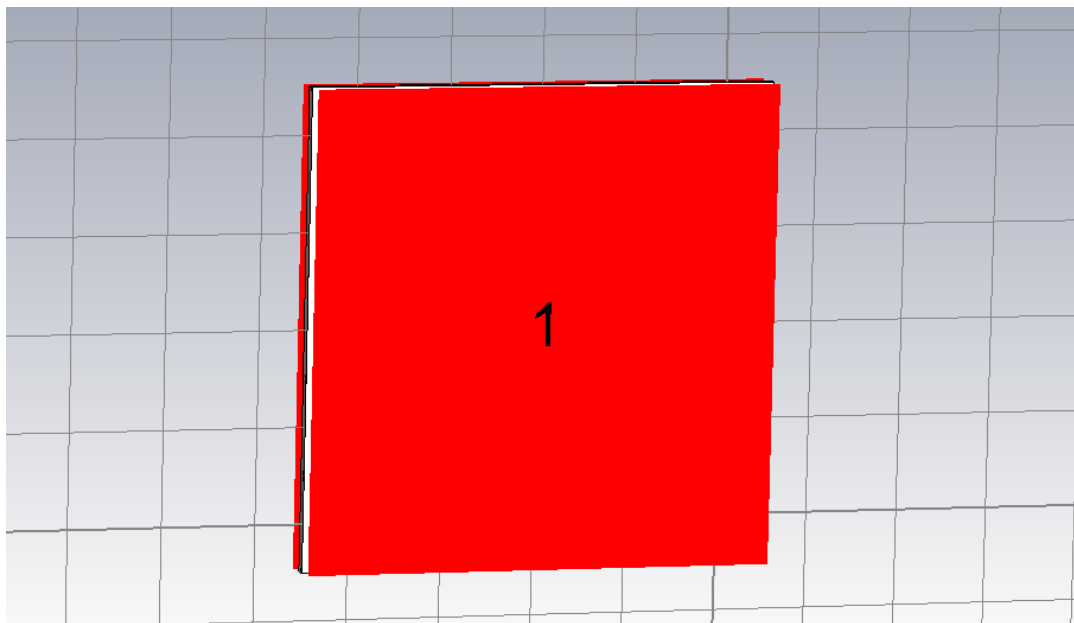
Fig. 4.12 Waveguide ports for the simulation
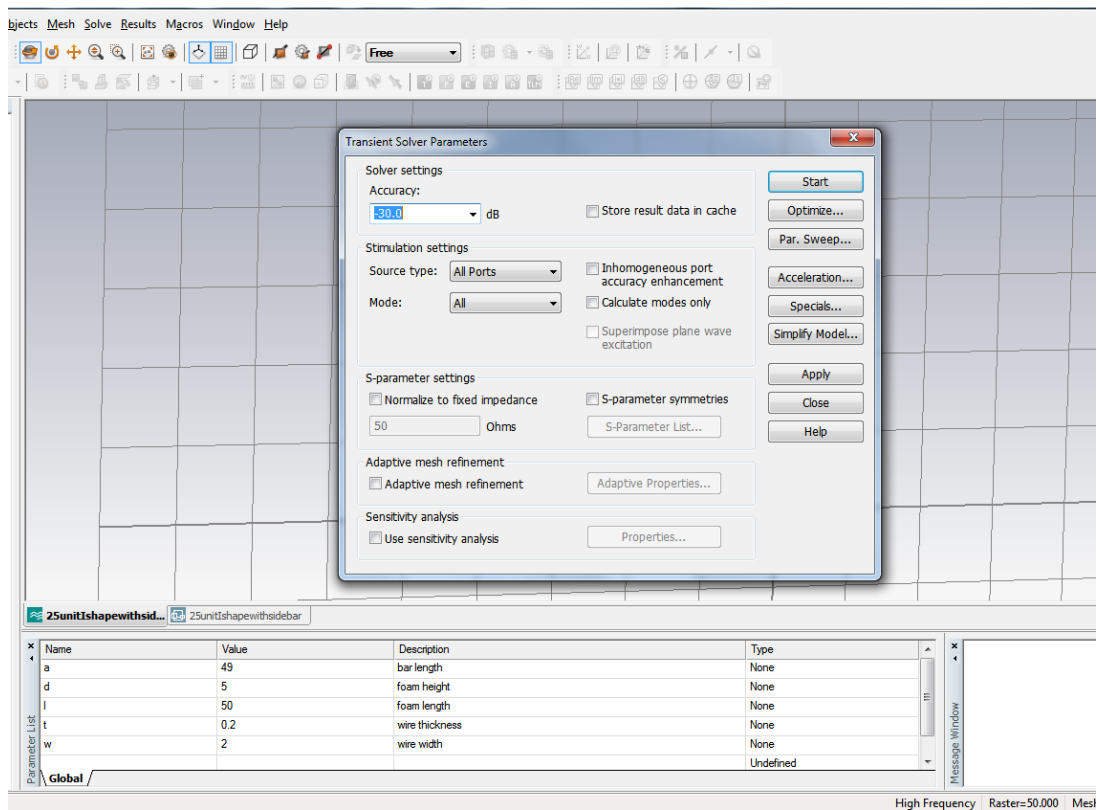
Fig. 4.13 Transient solver start

Following this design work, two waveguide ports are added to the structure with normally incident terahertz wave. The transient solver is then ready to set up and a number of simulations on the performance of the material interacting with in coming done and analyzed and discussed in the following chapters.

Chapter

5. PARAMETER RETRIEVAL AND ANALYSIS

5.1 I shape structure parameter optimization

5.1.1 Analysis for unit size (L value)

First the difference of the resonant frequency between different sizes identified by L of the unit cell from 30 by 30 um to 70 by 70 um is investigated. All the other parameters such as the gap distance, the wire width and the substrate thickness are kept the same. The resonant frequency is represented by the transmission plot S21 where the peak value of each curve is with the resonant frequency, as it is shown in Fig. 5.1.
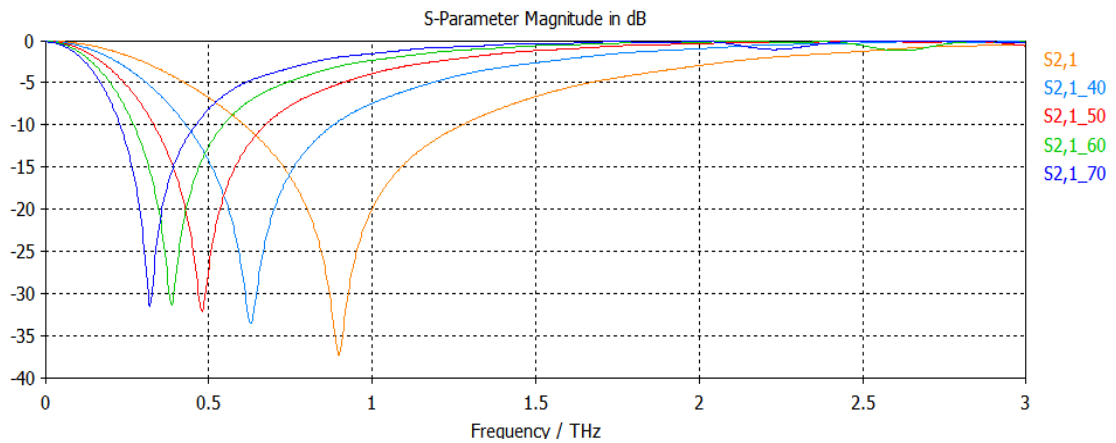
Fig. 5.1 S21 of the structures with different size of the unit cell
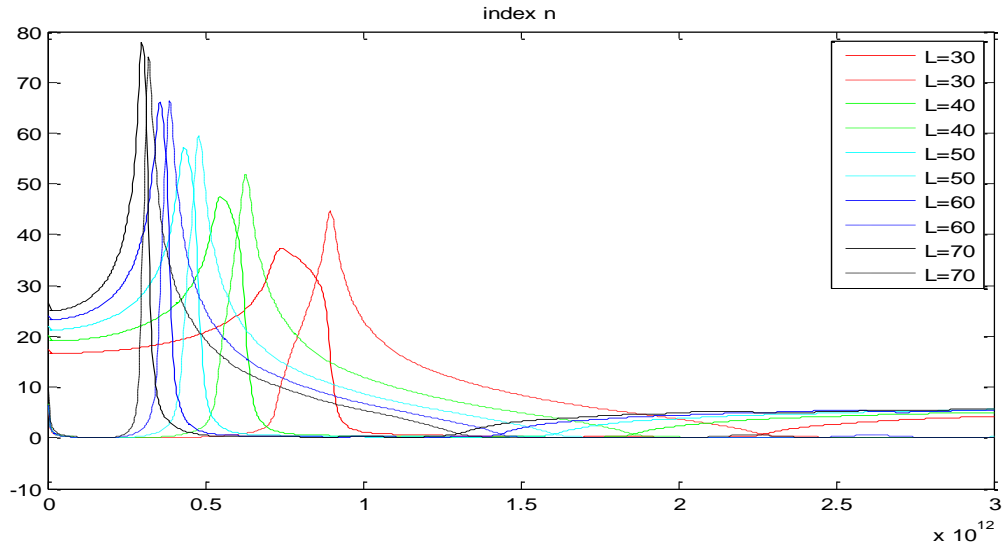
Fig. 5.2 Refractive index of the structures with different size of the unit cell

Fig. 5.2 shows the retrieved refractive indexes of the metamaterial for different L values. The solid line represents the real part of the refractive index while the dashed line represents the imaginary part of the refractive index. From the figure it can be concluded that as the size of the unit cell increases, the resonance frequency of the structure goes down and the index value is high. Also, for smaller the unit cell size, the refractive index band is broader around the resonance frequency (Fig. 5.2). The electrical permittivity and the magnetic permeability with respect to the cell size have the same trend as refractive indices, and are shown in Fig. 5.3. The larger the size of the unit cell the lower is the resonant frequency but has higher permittivity and permeability values. So with the smaller size of the metamaterial, the resonant strength becomes weaker and the resonant frequency becomes higher. This is could be due to the fact that at lower cell sizes, the interaction of the cell material with the incident wave is also less for both the metallic structure and the substrate foam so there exists less resonant particles in the material. For ease in fabrication and as well as characterization an optimum cell should be when L=50 um.
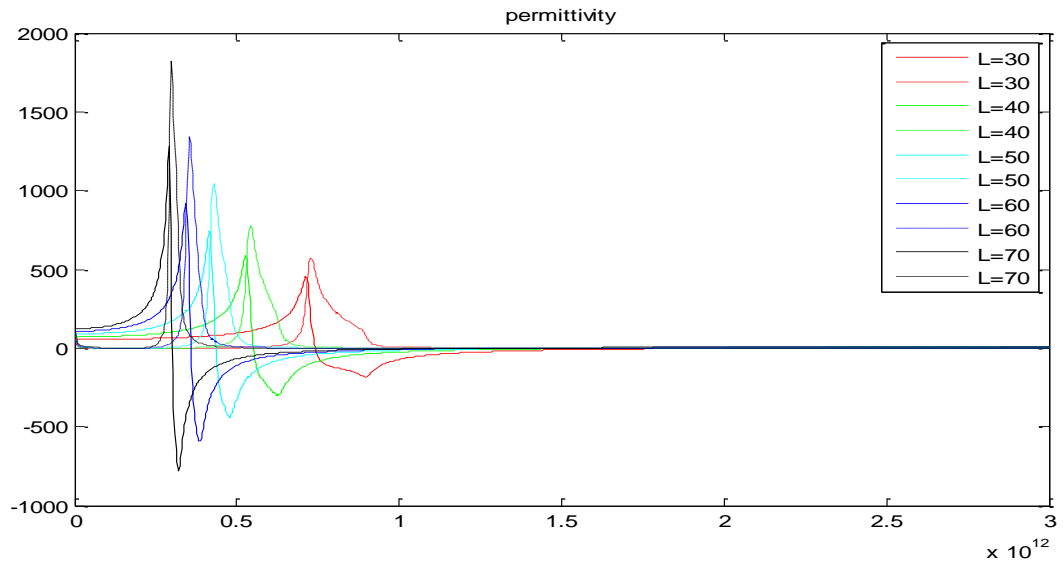
53

Fig. 5.3 Permittivity of the structures with different size of the unit cell
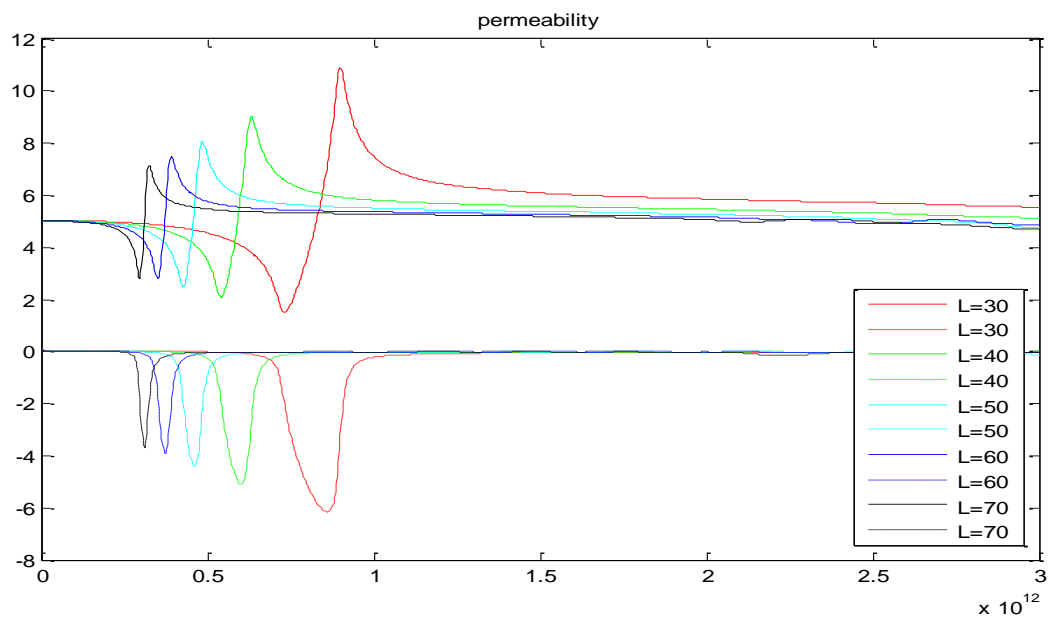

Fig. 5.4 Permeability of the structures with different size of the unit cell
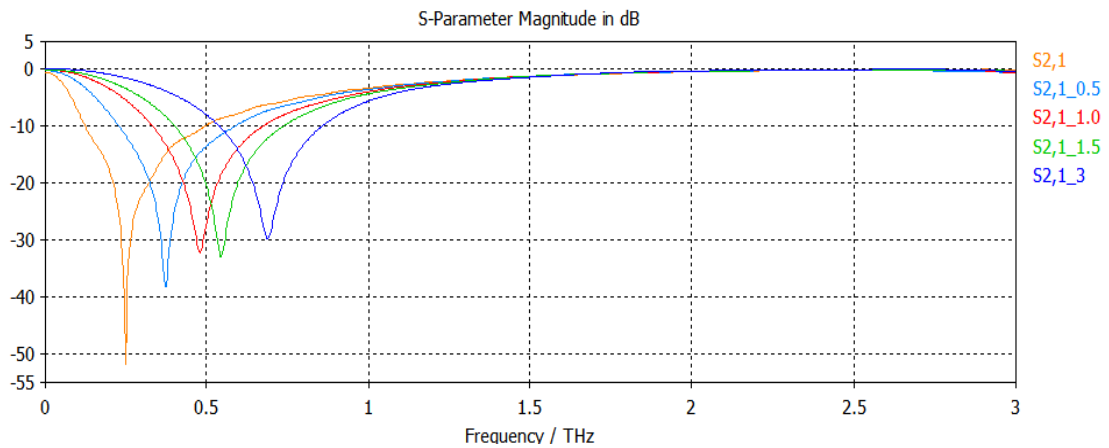
5.1.2 Analysis for gap distance, D

Fig. 5.5 S21 of the structure with different gap distance

It is of interest to determine the response of the structure for an optimized cell when the gap between the cells changes. In the simulations the difference in the resonance frequency when gap distances between unit cells were varied was studied, specifically the gap distance (G) was varied from 0.2 um to 3 um. All the other parameters such as the wire width and the substrate thickness were kept the same for a unit cell of L=50 um. The resonant frequency is represented by the peak value of each curve as shown in Fig. 5.5.
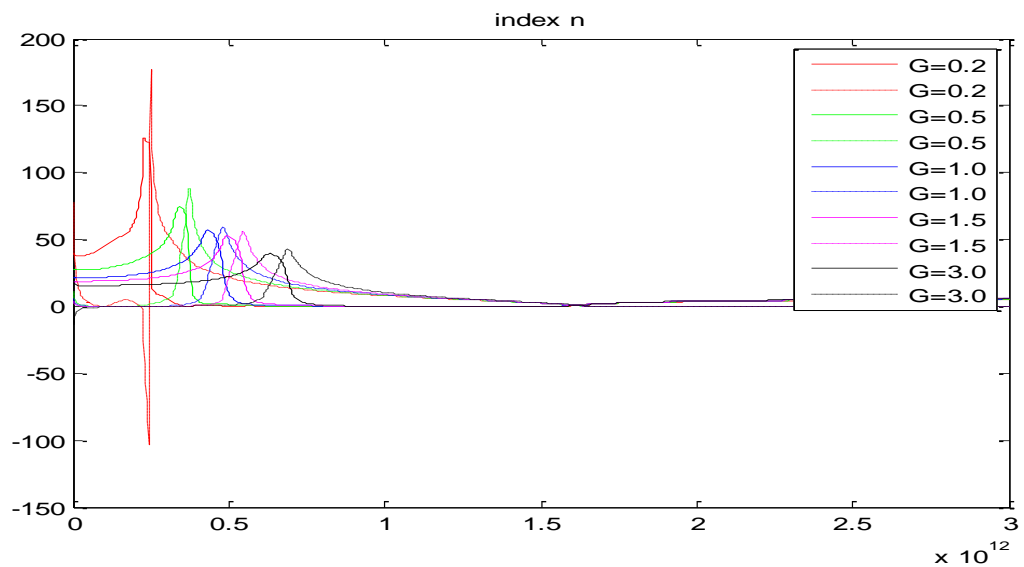
Fig. 5.6 Retrieved index of the structures with different gap distance

Fig. 5.6 shows the retrieved refractive indexes of the metamaterial with different gap distance between the unit cells. The solid line represents the real part of the refractive index while the dashed line represents the imaginary part of the refractive index. It can be concluded that the larger the distance between the unit cells, the higher is the resonant frequency. As the same time, the larger the distance between the unit cells is, the lower is the index value. This phenomenon could be attributed to the change of the capacitive resonance between the gaps since the closer the gap is, the stronger the electric response is between the gaps.

The corresponding electric permittivity and the magnetic permeability for the G distances follow the same trend as the refractive indices, as shown in Fig. 5.7 and Fig. 5.8. For large G, the resonance frequency increases while permittivity and the permeability values go down. So with the smaller distance between the gaps, the resonant strength becomes stronger and the resonant frequency becomes lower. However, in case of the permeability of the structure, is the two structures are too close to each other, the permeability becomes negative and the structure behaves like each unit is connected. It may be noted that when the gap is too small, it would be difficult to fabricate so for practical reasons, it is suggested that G=1 um should be chosen as the optimum gap distance.
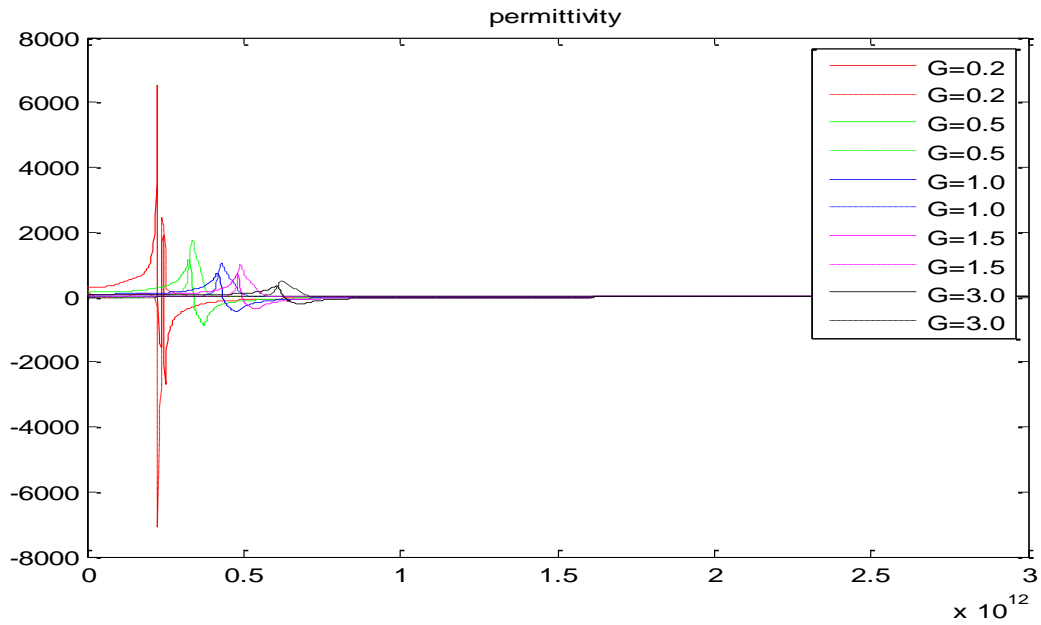
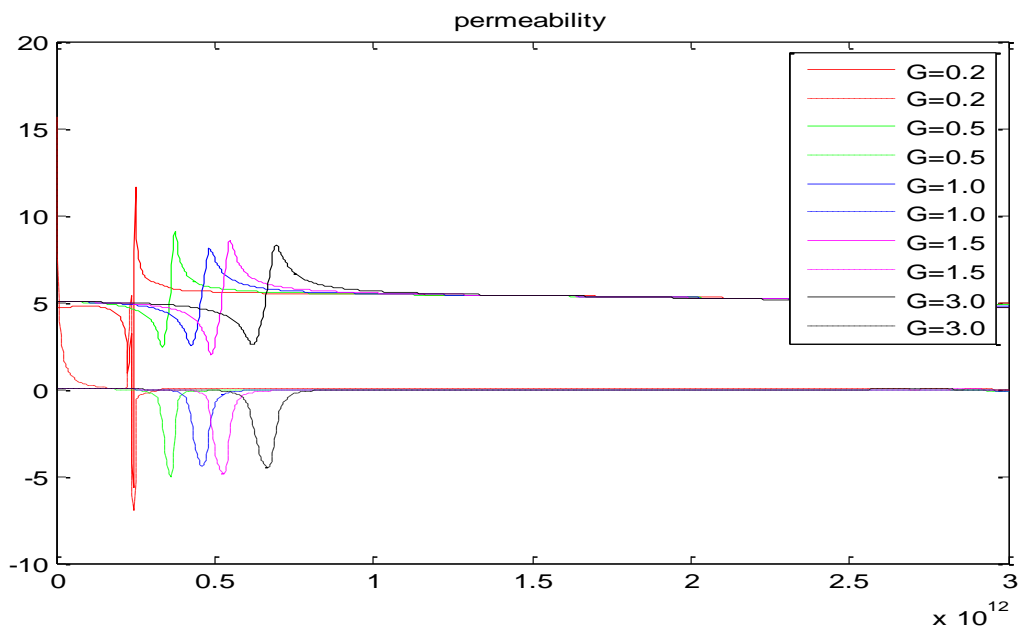Fig. 5.7 Permittivity of the structure with different gap distance

Fig. 5.8 Permeability of the structure with different gap distance

5.1.3 Analysis for unit width, W

Now is the difference of the resonant frequency between different wire widths of

the metallic structure which is identified by W from 0.5 um to 3 um. All the other

parameters are kept the same such as the unit size and the substrate thickness and the gap distance between the unit cells is kept with 1 um. The resonant frequency is represented by the peak value of each curve shown in Fig. 5.9.
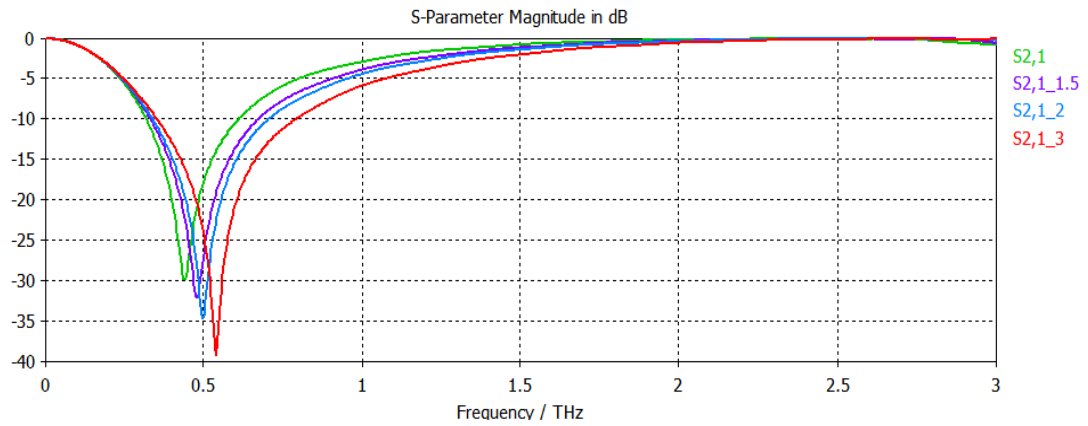

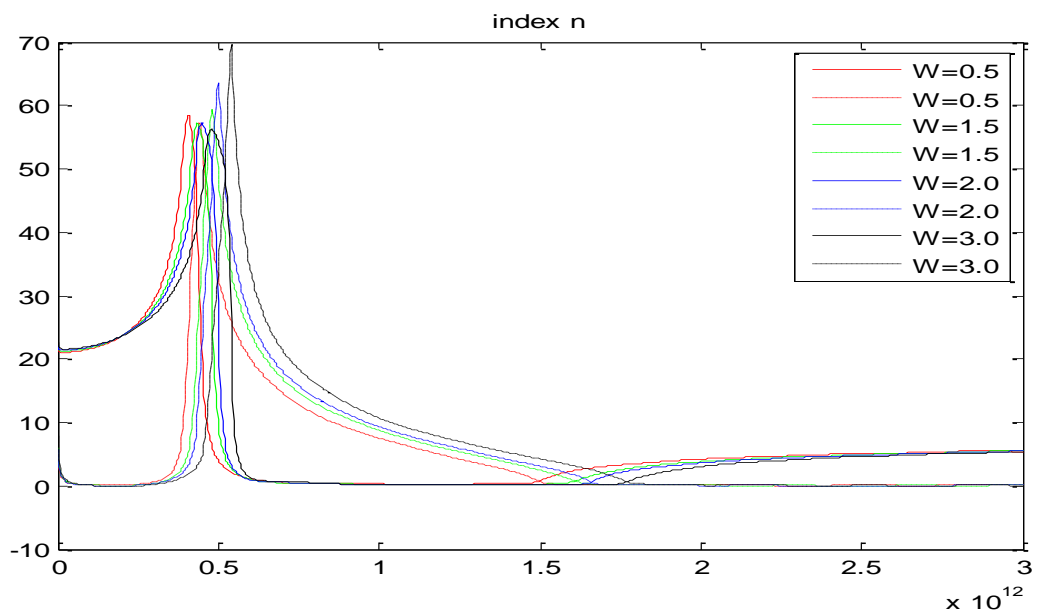Fig. 5.9 S21 of the structures with different wire width

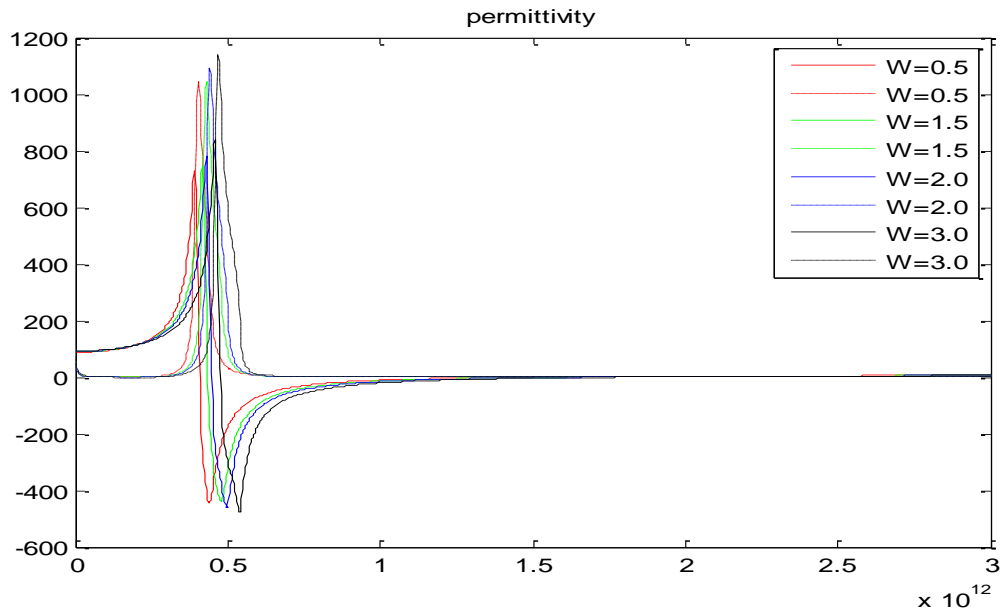Fig. 5.10 Retrieved index of the structures with different wire width

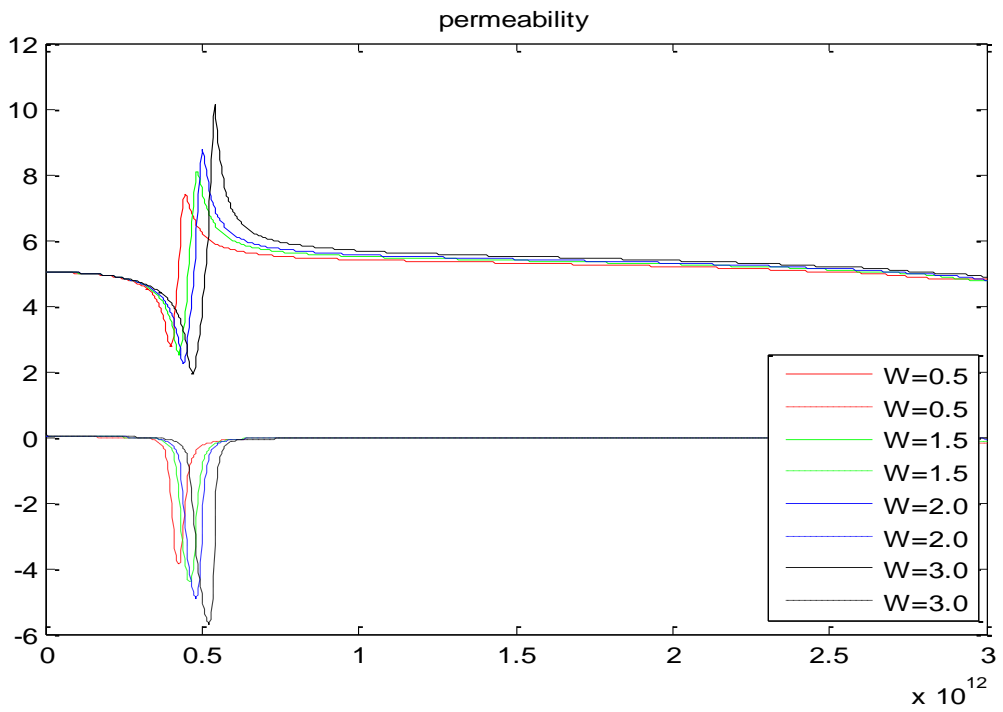Fig. 5.11 Permittivity of the structures with different wire width

Fig. 5.12 Permeability of the structures with different wire width

As shown from Fig. 5.10, the retrieved refractive indexes of the metamaterial with different wire width do not show a big difference in the operating frequency range. There is a slight shift in values but for most of the case, the resonant frequency and the index value are close to each other. The solid line represents the real part of the refractive index while the dashed line represents the imaginary part of the refractive index.

As for the corresponding electric permittivity and the magnetic permeability, it has the same trend of the values as that of the refractive index as shown in Fig. 5.11 and Fig. 5.12. The values for the permittivity do not change a lot with wire width and the resonant frequency only shift a small amount along the operating frequency. However, there is a change in the value of the permeability for the structure. The wider is the wire; the lower is the permeability. The more the magnetic moment is increased, the more magnetic response is canceled which is caused by the incident wave. This is consistent with the observations of J. T. Shen's research in 2009 [18].
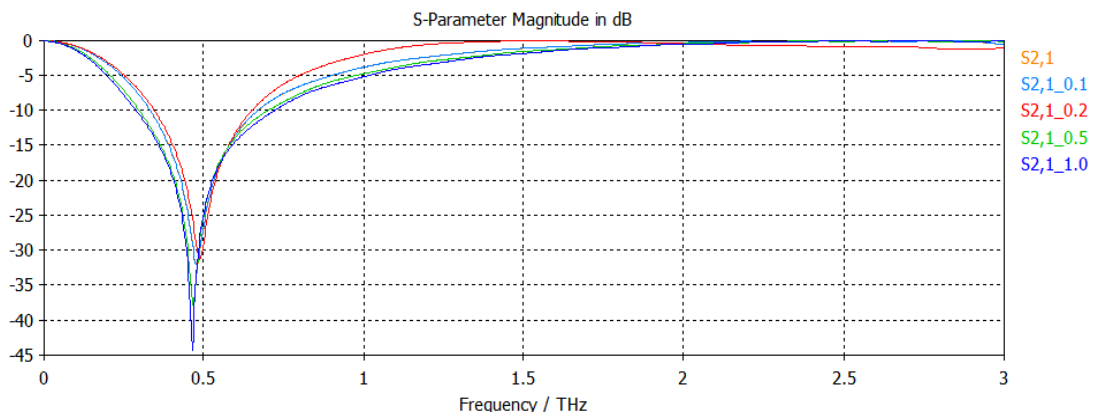
5.1.4 Units with different metal thickness, T

Fig. 5.13 S21 of the structures with different metal thickness

60

The effect of the metal thicknesses embedded in the unit cells were studied next. The thickness is defined through the parameter T which was varied from 0.01 um to 1 um. All other parameters were kept the same such as the unit size and the substrate thickness and the gap distance between the unit cells. The resonant frequency is measured through the transmission plot S21 at the peak value of each curve as shown in Fig. 5.13.

As shown in Fig. 5.14, the retrieved refractive indexes of the metamaterial with different metal thickness do not show any big difference in the operating frequency range. The index values of different thicknesses are almost the same and the resonant frequency does not shift at all. In the figure the solid line represents the real part of the refractive index while the dashed line represents the imaginary part of the refractive index.
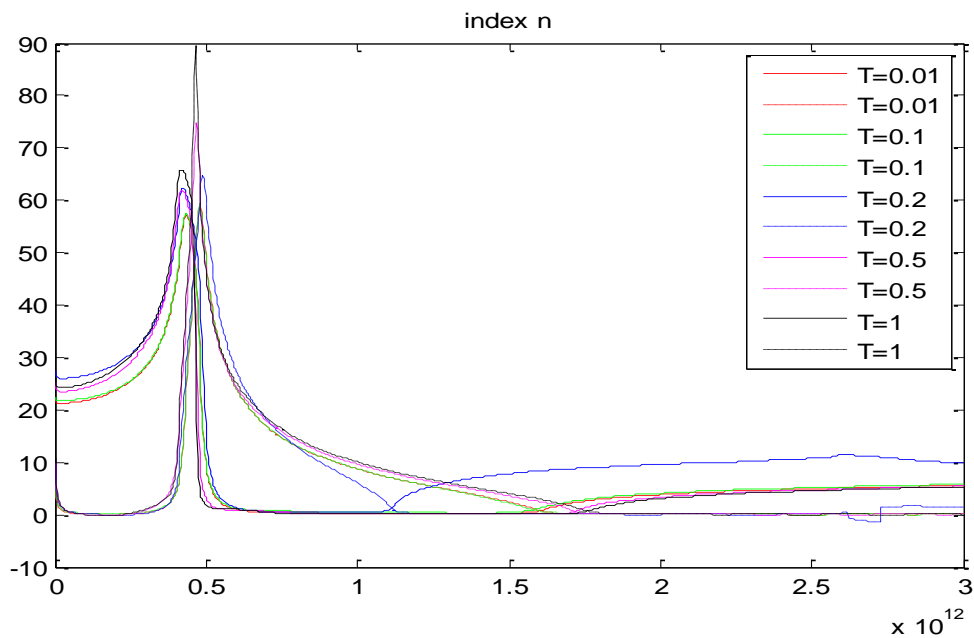

Fig. 5.14 Retrieved index of the structures with different metal thickness

As for the electric permittivity and magnetic permeability of the structure, the trend is the same as that of the refractive index, as shown in Fig. 15 and Fig. 16. The values

do not change and the resonant frequency does not shift. It can be concluded that the thickness of the metal does not affect the materials electric and magnetic responses under electromagnetic fields.
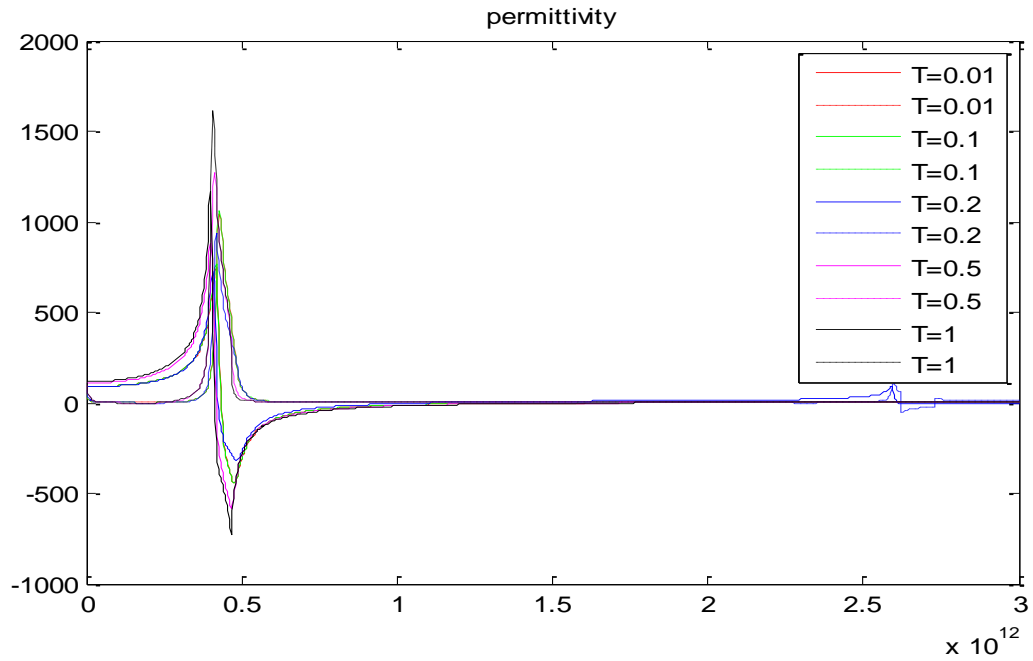

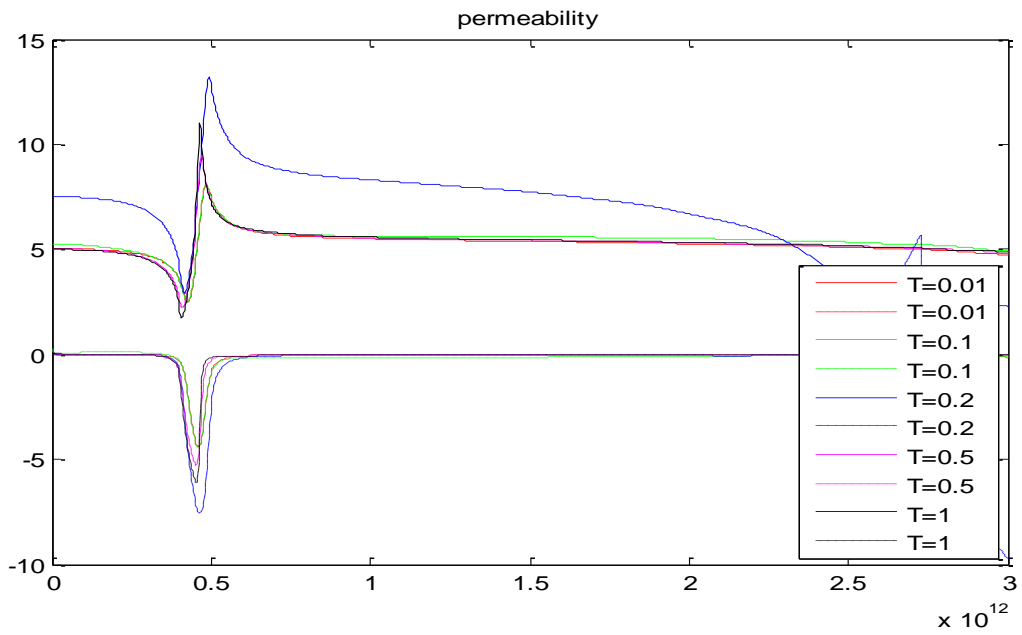Fig. 5.15 Permittivity of the structures with different metal thickness

Fig. 5.16 Permeability of the structures with different metal thickness

5.1.5 Units cells with different substrate thickness, D

Finally, the difference of the resonant frequency of the unit cells with different substrate (slab) thicknesses thickness t was identified by the parameter D, which varied from 2 um to 15 um. All the other parameters are kept the same such as the unit size and the wire width and the gap distance between the unit cells. The resonant frequency is represented by the peak value of each curve as shown in Fig. 5.17.
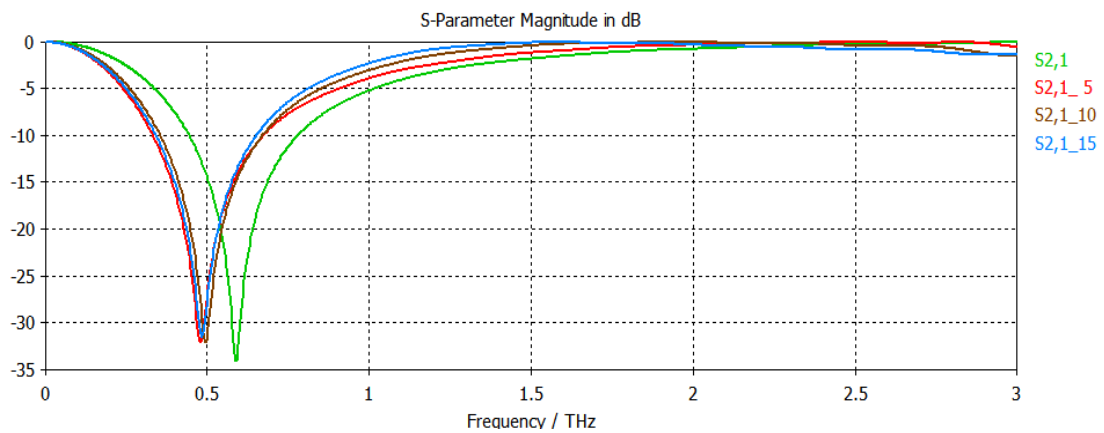

Fig. 5.17 S21 of the structures with different substrate thickness

As shown from Fig. 5.17, the resonant frequency of the metamaterial with different substrate thickness do not show noticeable difference in the operating frequency range. The values of transmission for different thicknesses are almost the same and the resonant frequency does not shift at all except for the one that is really thin and the average could be considered unchanged.
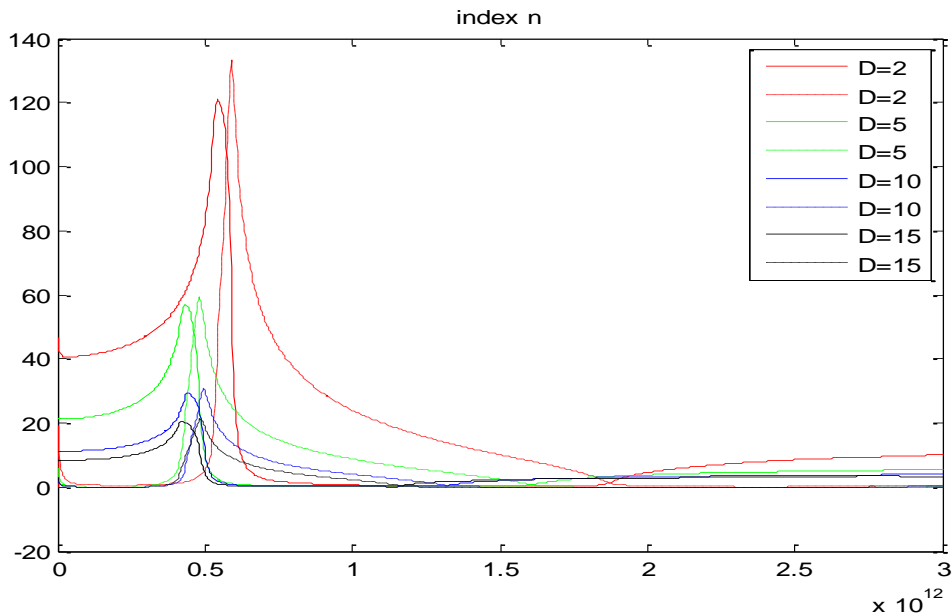
Fig. 5.18 Retrieved index of the structures with different substrate thickness

The retrieved refractive indexes of the metamaterial with different substrate thicknesses are shown in Fig. 5.18. It's clear from the plot that the index values changes a lot due to the thickness of the substrate while the resonant frequency does not shift a lot. The thinner the substrate, the higher is the refractive index value. This is mostly due to the retrieval method which uses the thickness as the denominator in the formula (Equation 5 and 6) [18]. The solid line represents the real part of the refractive index while the dashed line represents the imaginary part of the refractive index.

As for the electric permittivity and the magnetic permeability, the trend is the same. The thinner the substrate is the higher value will be achieved. For the optimization and the fabrication flexibility, the thickness for 5 um is chosen as the standard sample.
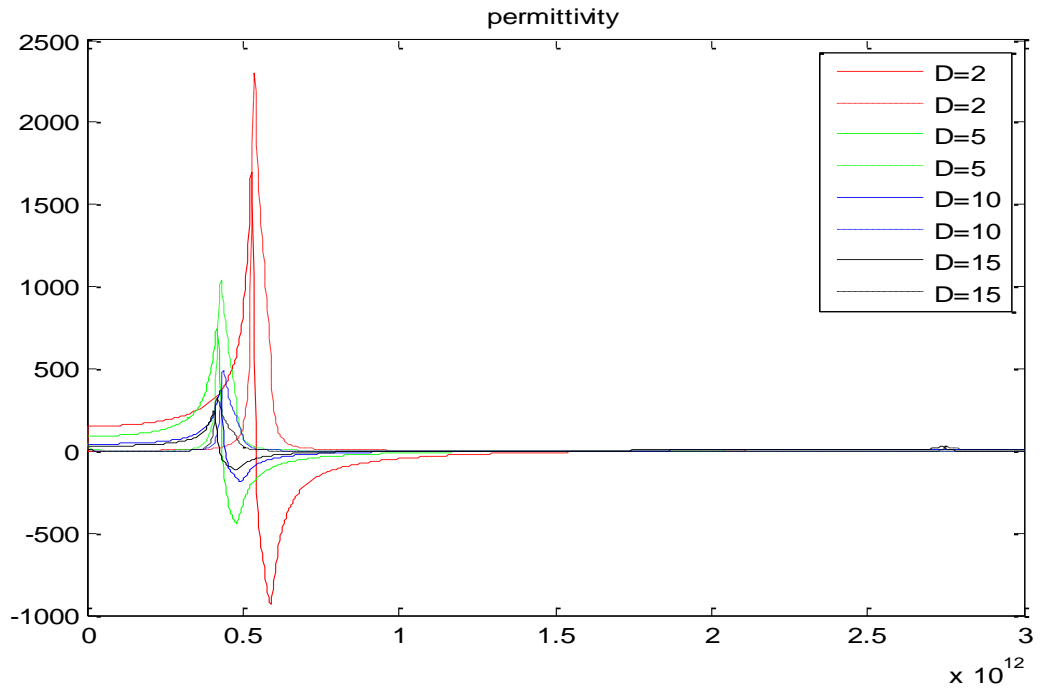
64

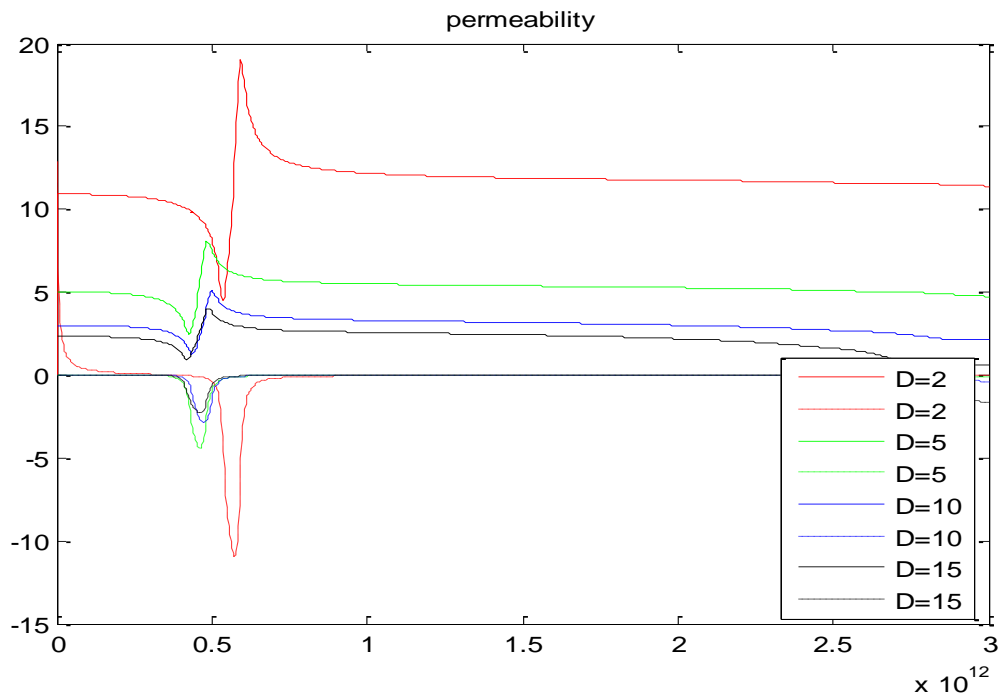Fig. 5.19 Permittivity of the structures with different substrate thickness

Fig. 5.20 Permeability of the structures with different substrate thickness

5.2 Dual band structure parameter optimization

In this section, the performance of the dual band structure and optimize the parameters of the design will be disclosed. As it is described before, the new dual band structure is based on the original "I" shape structure with two sets of cut wires added on the side of the center bar of the "I" shape structure. However, to get the best results with the highest value of the refractive index and widest band coverage, lots of characteristics need to be optimized such as the cut wire position, the gap between the cut wires and the cut wire's width.

As a comparison, the retrieved results of this dual band structure has a dual bands of resonant frequency compared to the single band structure. The added cut wires contribute the most to the second resonant frequency band. In this chapter, the main goal is to investigate how the cut wire will affects the second resonant frequency band.

5.2.1 Materials response to variation in side bar position

When adding the cut wires to the "I" shape structure, it's hard to know what the optimum position of the cut wires is. Analysis was therefore done by changing the position of the cut wires away from the center bar in fixed segment. The transmission plot for each design is shown in Fig. 5.21. It can be seen from the plot that since the cut wires define the second resonant frequency, the second resonant frequency changes with the change of the position of the cut wire. The resonance frequency moves from ~1.5 THz to 2 THz and then move back to 1.5 THz. Actually, the highest resonant frequency occurs at the medium position of the cut wire, where it is neither further or closer to the center bar. Once it is moving further or closer, the resonant frequency will shift lower.
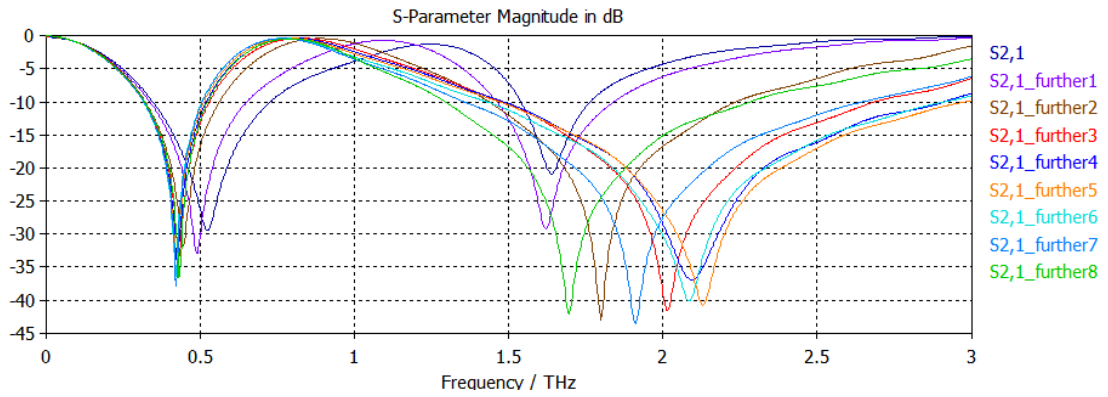
Fig. 5.21 S21 of the structures with different positions of the cut wires

The refractive index has the same trend as the transmission plot. The lower index band remains unchanged while the second index peak value shifts with changes in the position of the cut wires. The peak value of the refractive index shifts to a higher frequency and then reverts back to a lower value as the cut wires moving further from the center bar. The permittivity and the permeability move in the same way as the resonant frequency. However, the peak value of the permittivity and the permeability does not change a lot with different position of the cut wires. Thus the second high refractive index values are almost the same with different cut wire positions. Fig. 5.23 and Fig. 5.24 show the permittivity and the permeability of the simulated structure.
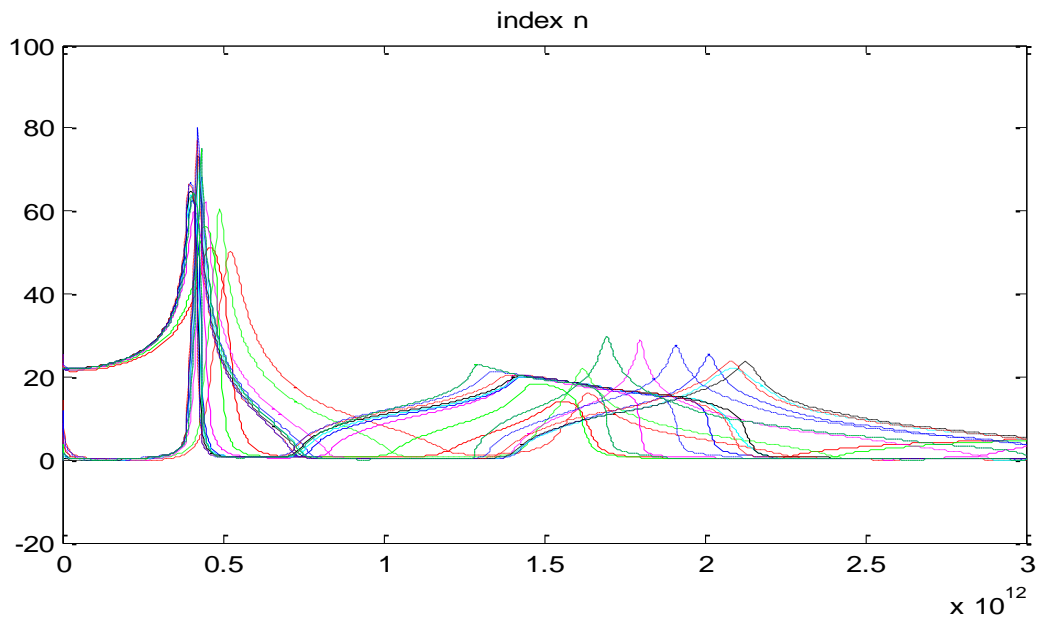
Fig. 5.22 Retrieved index for structures with different positions of the cut wire
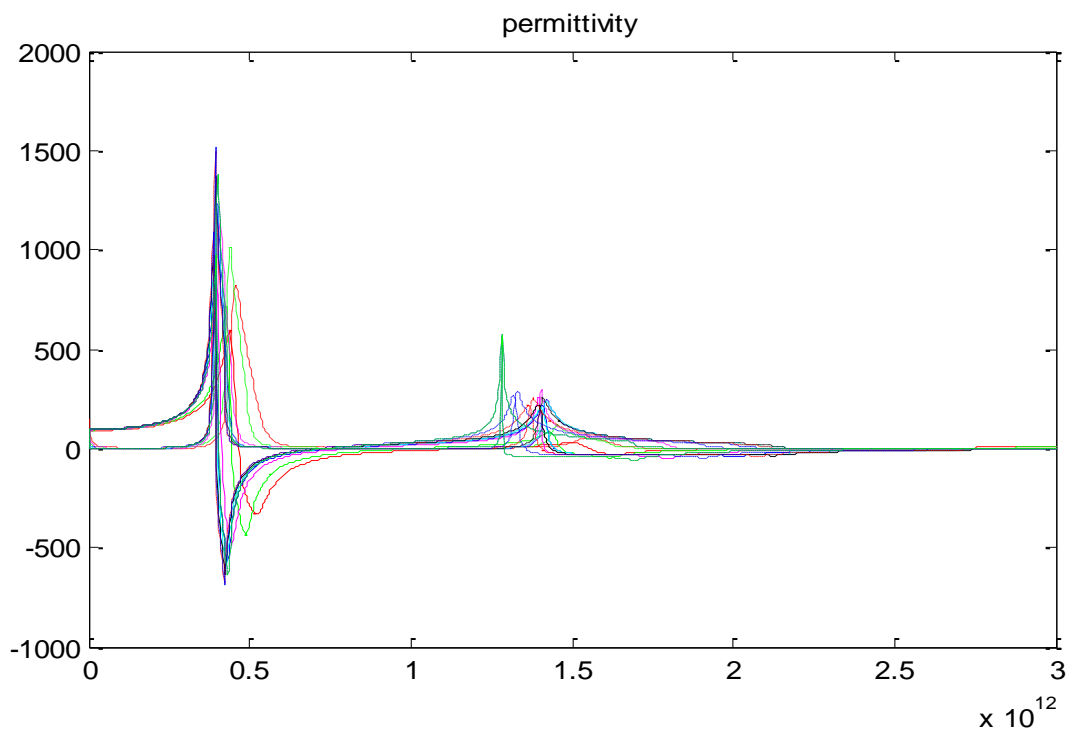

Fig. 5.23 Permittivity of the structures with different positions of the cut wire
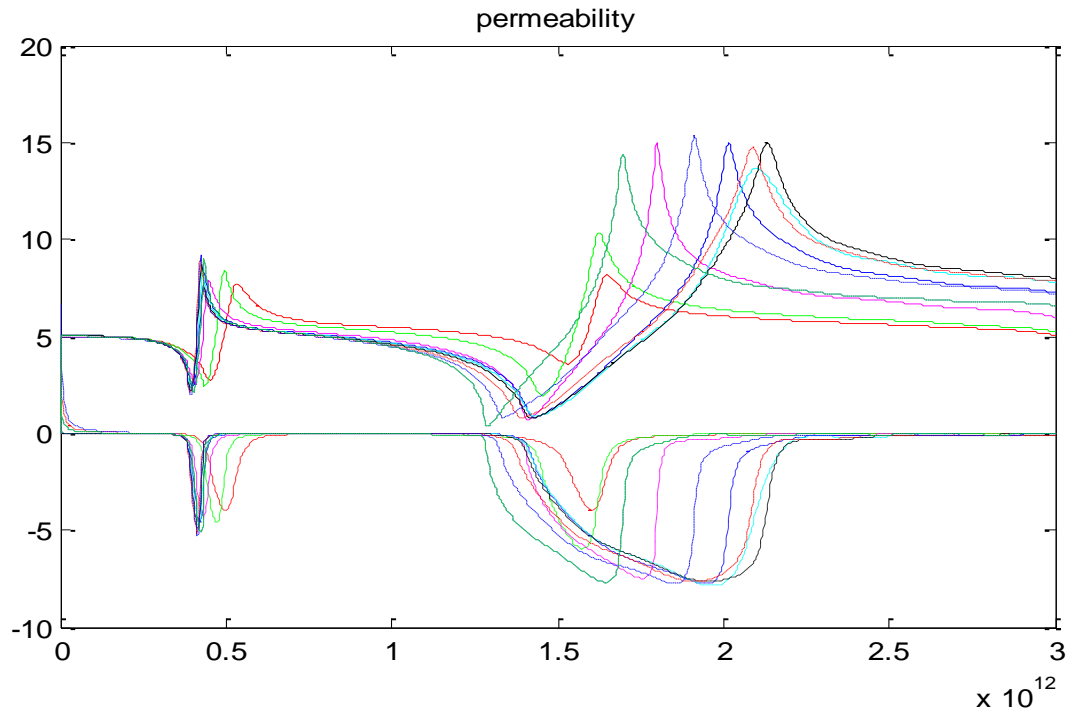
Fig. 5.24 Permeability of the structures with different positions of the cut wire

5.2.2 Different gap distance between the side bars

Since the electric response depends mostly on the capacitive resonance that exists in the structures, different gap distance between the cut wires as those between the unit cells need to be investigated to find the best performance of the metamaterial. Fig. 5.25 shows that there exists a big shift in the second resonant frequency with the gap between the cut wires increasing. The resonant frequency shift from near 1 THz to almost 3 THz with the gap changes from 0.2 um to 5 um.
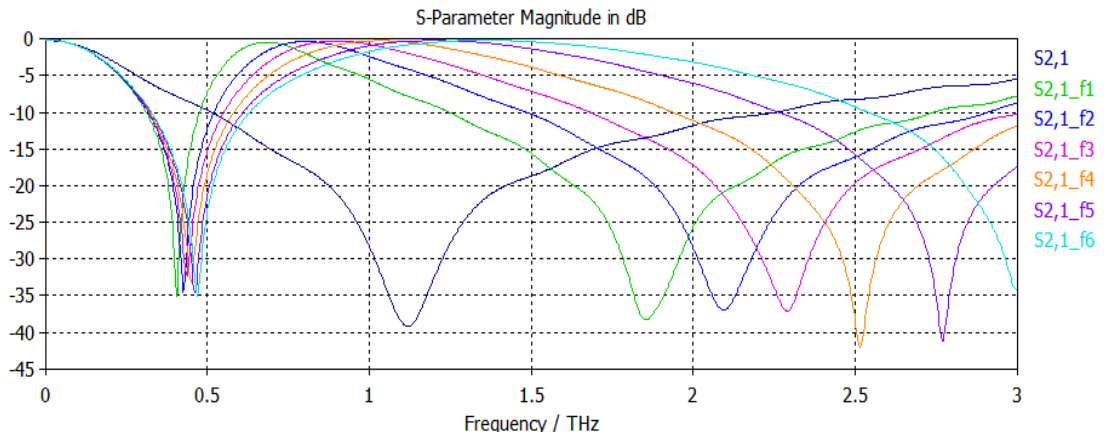
Fig. 5.25 S21 of the structures with different gap distance between the cut wires

The corresponding refractive index also changes with the change of the gap between the cut wires. With the gap becoming larger, the index value decreases slightly but the index value for the first resonant frequency does not change too much.
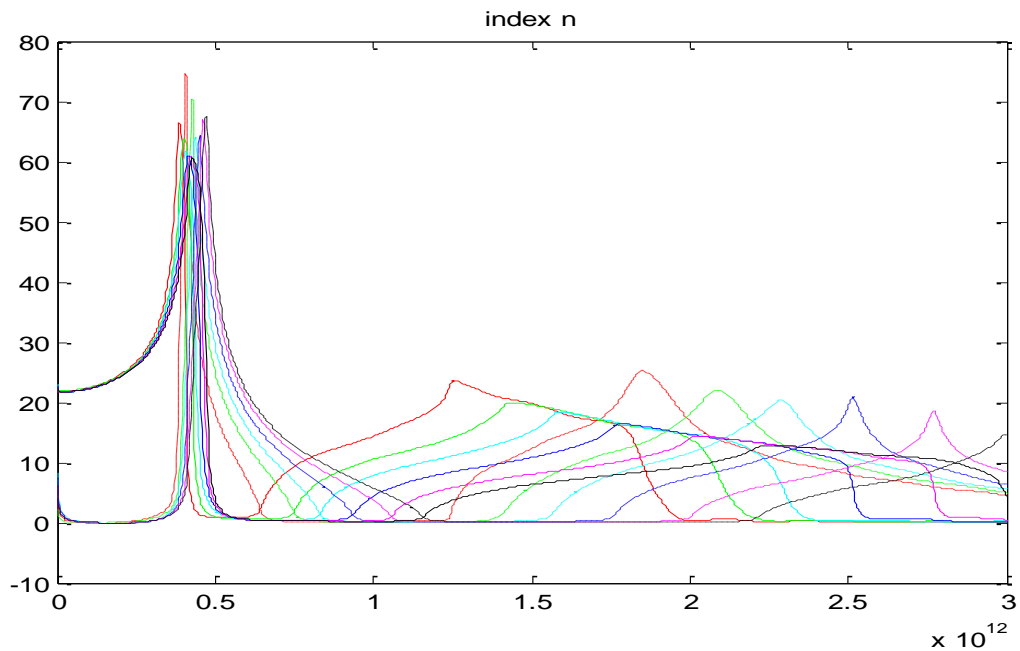

Fig. 5.26 Retrieved index of the structures with different gap distance between the cut wires

As shown in the plot, the electric permittivity of the material decreases sharply with the gap increases. So it verifies that the second resonant mainly come from the capacitive response between the gaps of the cut wires.
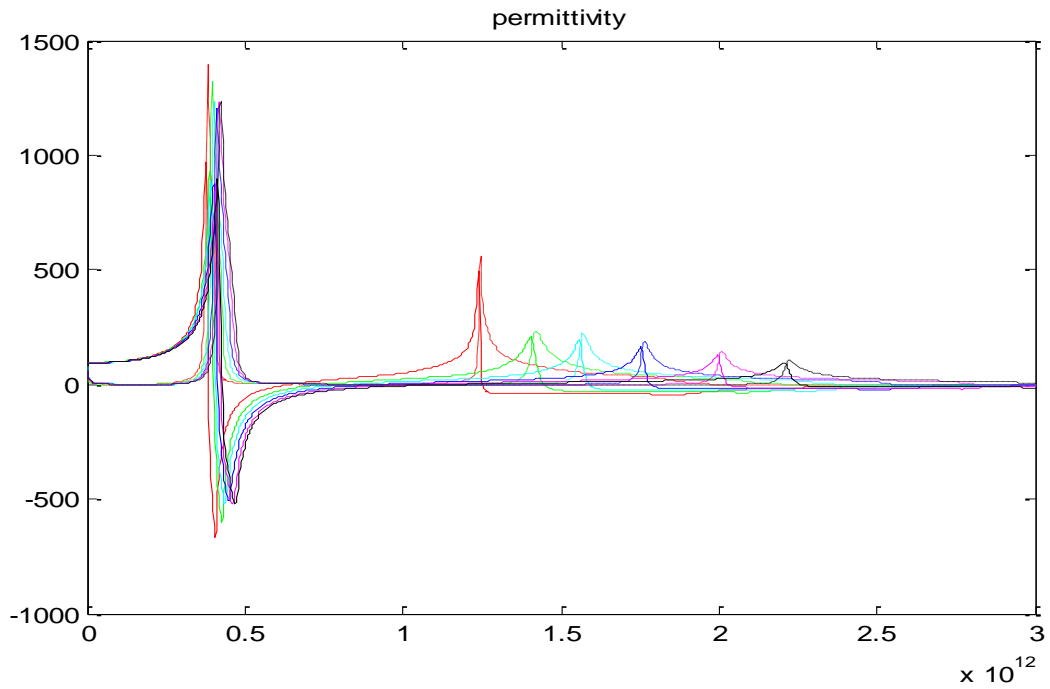

Fig. 5.27 Permittivity of the structures with different gap distance between the cut wires
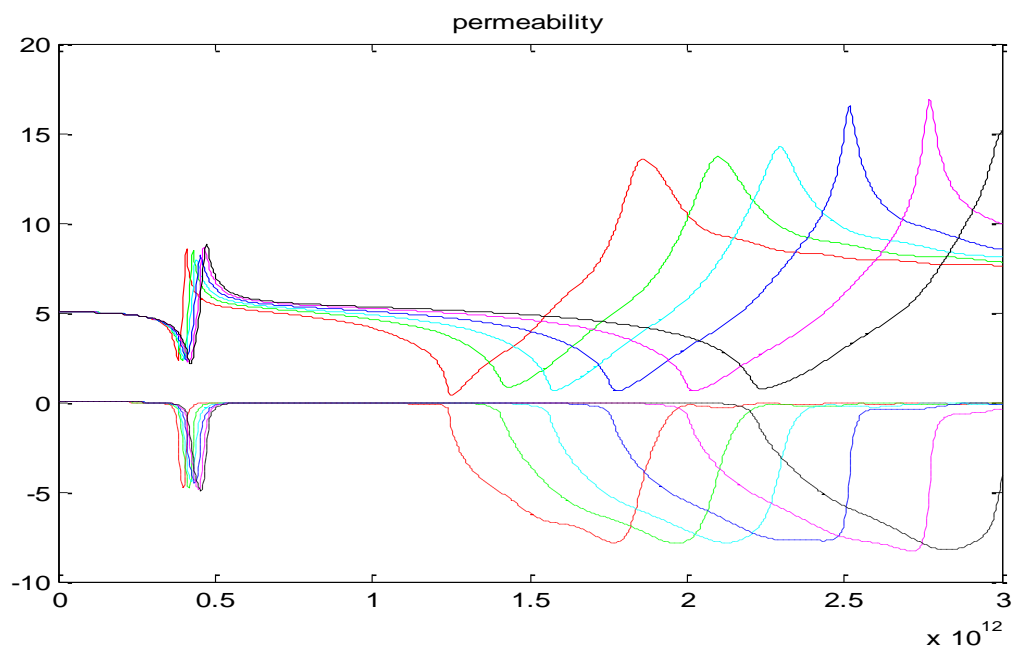

Fig. 5.28 Permeability of the structures with different gap distance between the cut wires

5.2.3 Different gap between unit cells

As what is done for the "I" shape structure, the performance of the material with different gap between the unit cells were investigated for the dual band structure as well. However, from the transmission plot and the retrieved parameters, it was evident that there was no big change with a change of the gap distance. The resonant frequencies are close to each other, the index values were close and so were the permittivity and the permeability values.
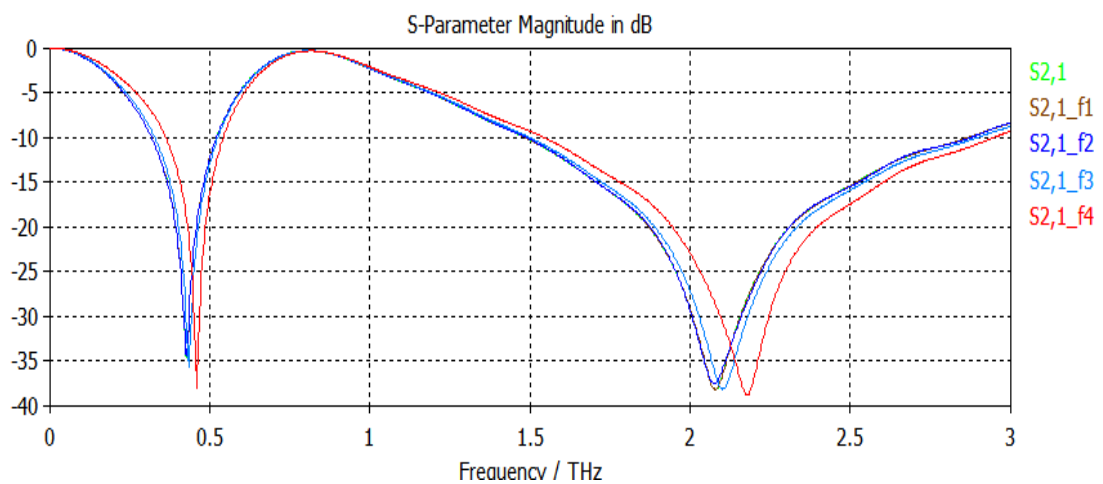
Fig. 5.29 S21 of the structure with different gap distance between the unit cells

In conclusion, the gaps between the unit cells do not affect the intrinsic parameters significantly in the dual band structure since the main resonance exist within the structure but not between the structures as is the case for the "I" shape structure.

Fig. 5.30 Retrieved index of the structures with different gap distance between the unit cells

Fig. 5.31 Permittivity of the structures with different gap distance between the unit cells

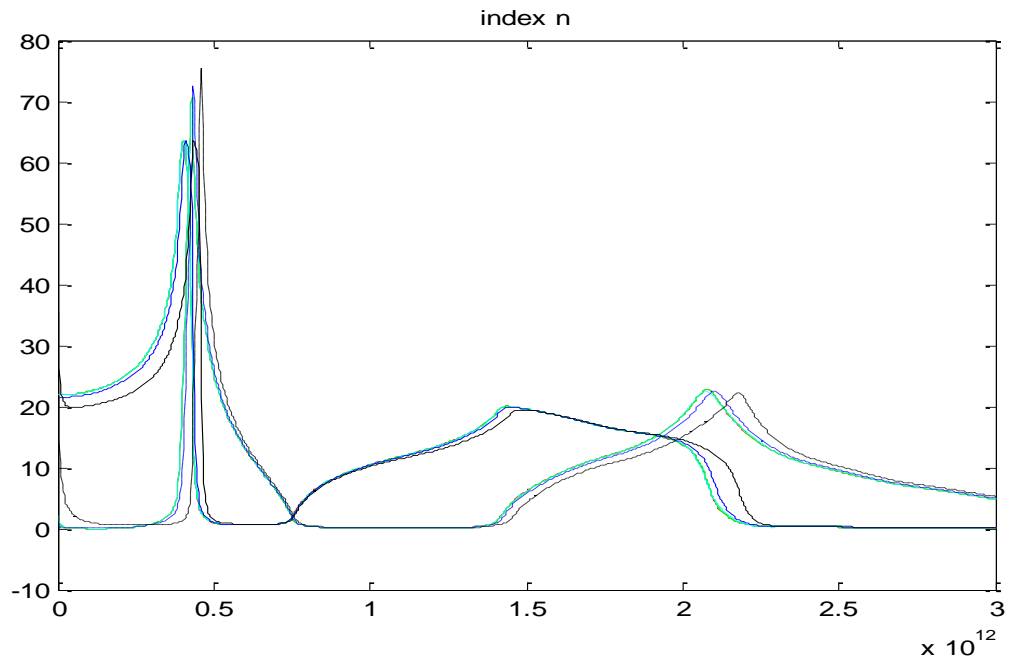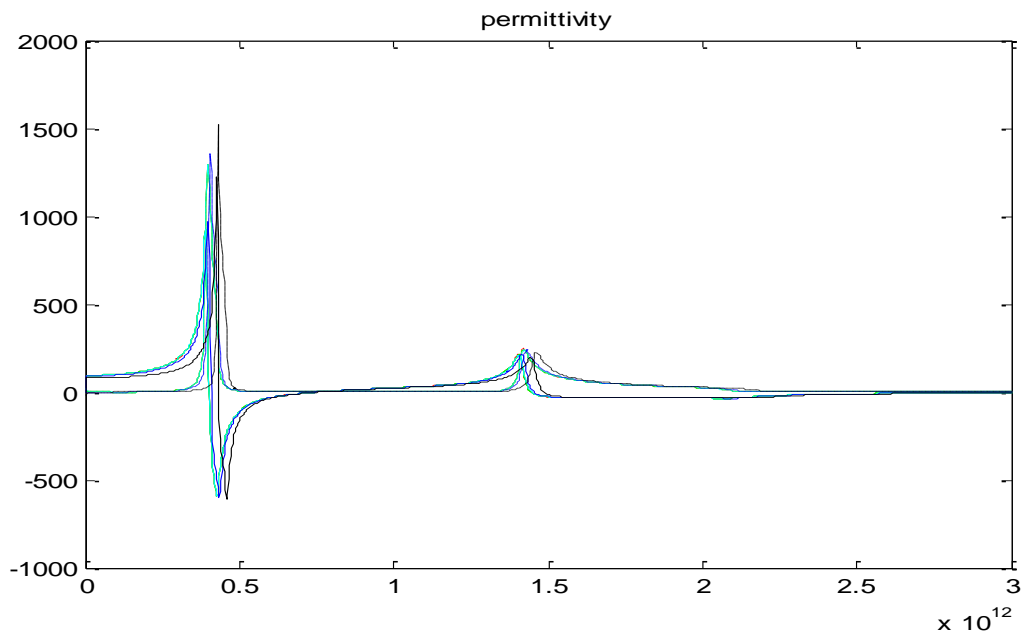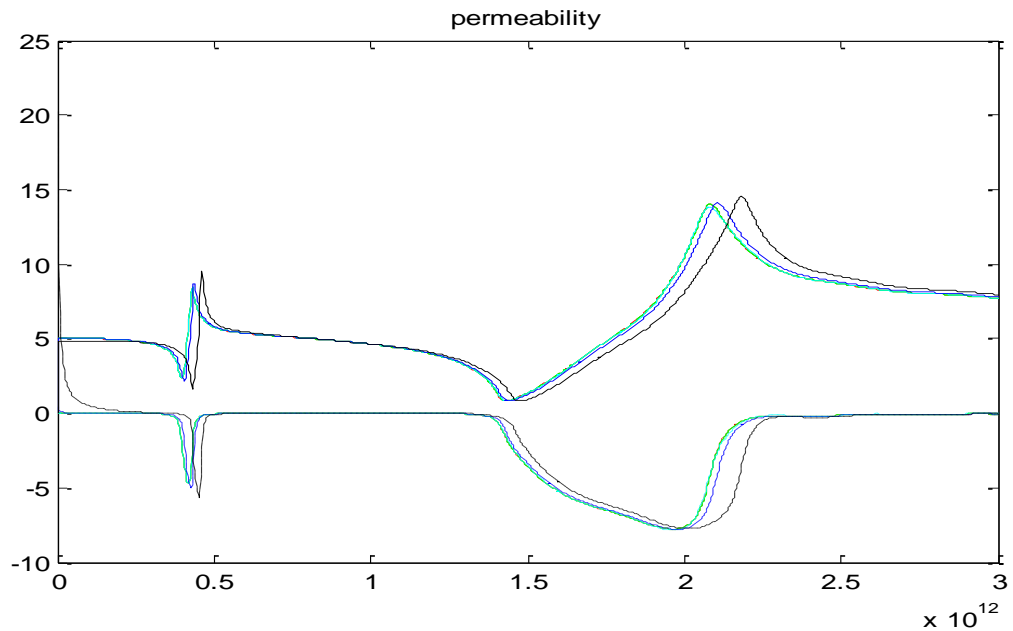Fig. 5.32 Permeability of the structures with different gap distance between the unit cells

5.2.4 Parameters with different sidebar width

In this concluding section the different performance of the structure with different cut wire width is investigated since the width of the wire will affect the magnetic moment in the structure. As it is shown from the simulation result, the resonant frequency is affected by the width of the cut wires but the effect is not as significant as that in the "I" shape structure. The permittivity is not affected much and the magnetic permeability is also not affected much by the width of the cut wires. Since the current loop on the cut wires are in the same direction and the two sets of magnetic moment might cancel with each other, with the result that the magnetic moment is not affected much by the cut wires. So the value of the permeability does not change but the resonant frequency shifts due to the change of the quantity of the metal material with the width change.
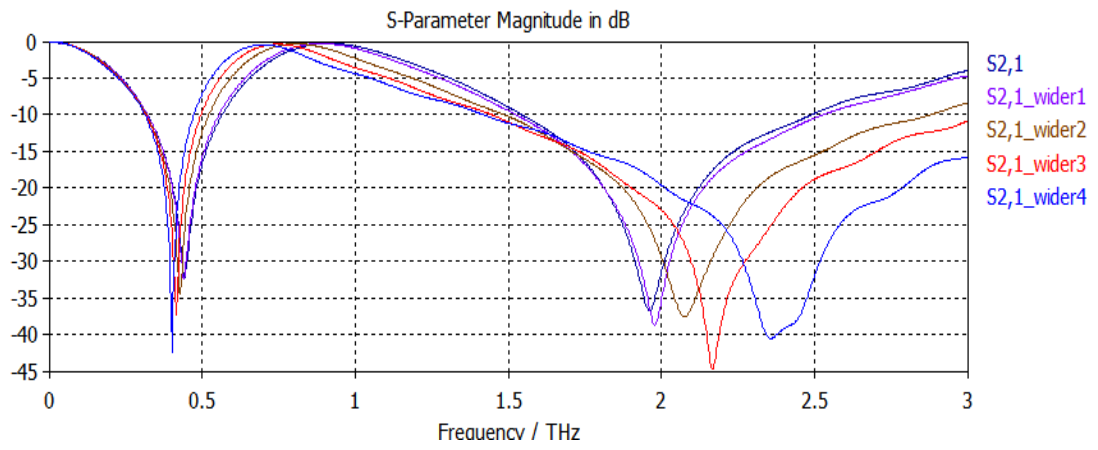
74

Fig. 5.33 S21 of the structures with different cut wire width
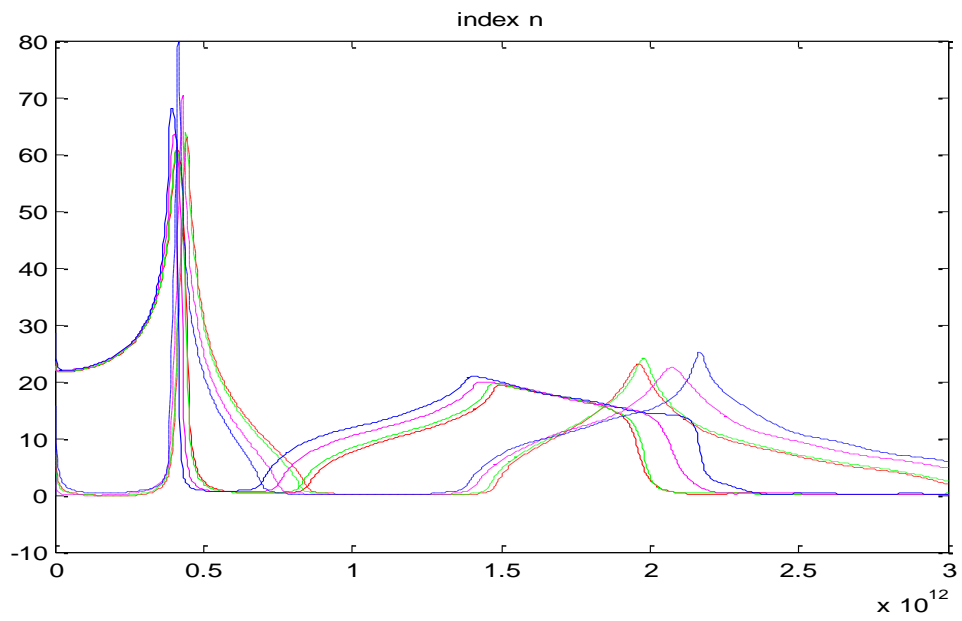

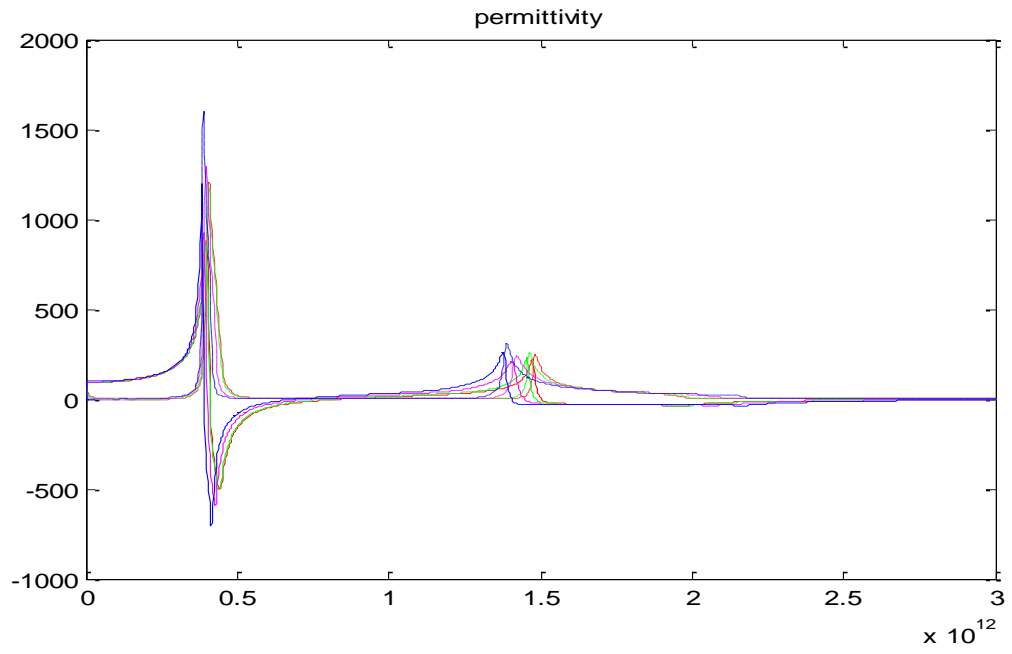Fig. 5.34 Retrieved index of the structures with different cut wire width

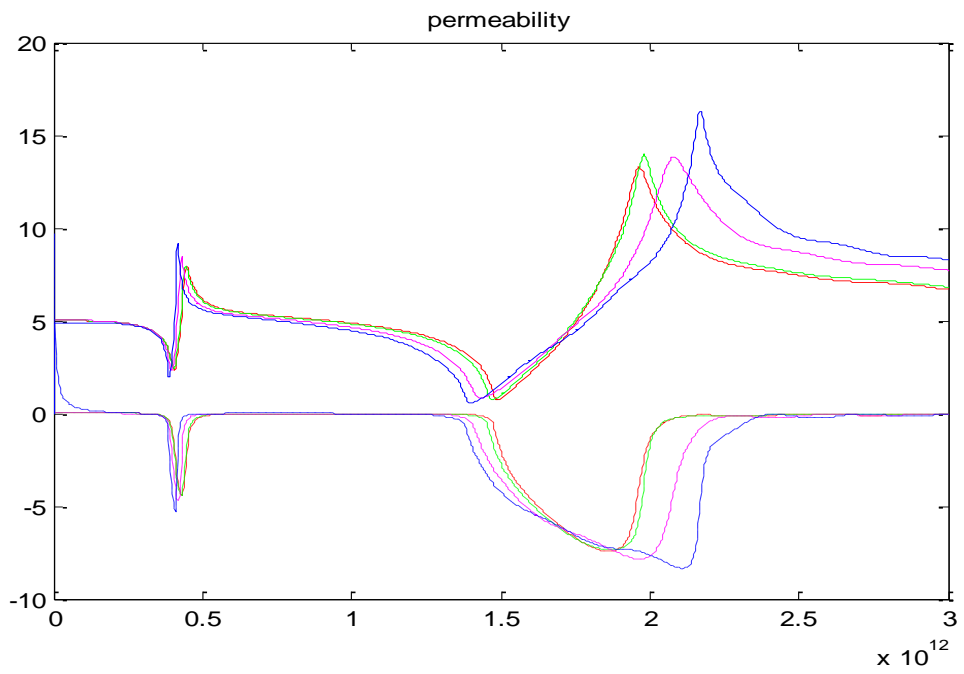Fig. 5.35 Permittivity of the structures with different cut wire width

Fig 5.36 Permeability of the structures with different cut wire width

Chapter

6. CONCLUSION

A metamaterial structure with ultra-high refractive index values at two frequency bands was successfully designed. The dual refractive index, dual frequency structure was based on a single frequency structure with additional components to generate high refractive index at the second frequency band.

First, the single band structure was verified and optimized for the target frequency range. In the optimization process, the optimized parameters such as unit size, unit thickness, unit distance and wire width of the structure were defined to achieve the best refractive index value that can be achieved in the designed frequency range. Based on the optimized single band structure, by adding two bars on the side of the center bar, a dual band structure could give two resonant frequencies.

The dual band design which has two resonant frequency bands, is a great improvement compared to the single band structure. As discussed in chapter 5, by optimizing the parameters of the dual band structure such as the side bar position, the width of the side bar, the gap between the side bars and the distance between the units, an optimized value of the refractive index at the second resonant frequency is achieved. From the analysis in the second part of chapter 5, it's clear to see that the peak refractive index value at the second band is much higher than that of a natural material, although it is not as large as that at the first resonant band. This second resonant band can be considered as a broad band which covers over 1 THz with a refractive index above 10, which could bring a broad range of application in which multiple resonant bands with high index are required.

This new broad band dual resonant frequency high refractive index metamaterial has potential applications in a lot of area where requires a multiple frequency response. Since it cover two broad band with high index values, there's no need to produce two separate devices for different frequency requirements. It provides more convenience and flexibility of manufacturing the equipment.

The future work includes the fabrication of the device and measurement of its properties. Nano fabrication techniques need to be applied and the advanced THz-TDS measurement method is going to be used for the experiment on the real product. The experiment results will be compared to the simulation results and the material will be tuned up to the best configuration.

REFERENCE

[1] J. Taylor, J. Morwood, "Pocket Oxford Classical Greek Dictionary," ISBN-13: 978-0198605126

[2] Veselago V. G. "The electrodynamics of substances with simultaneously negative values of ε and μ," Sov. Phys. Usp. 10, 509–514 (1968)

[3] J. B. Pendry, A. J. Holden, D. J. Robbins and W. J. Stewart, "Magnetism from conductors and enhanced nonlinear phenomena," IEEE Trans. Microwave Theory Tech. 47, 2075 (1999)

[4] B. T. Schwartz and R. Piestun, "Total External reflection from metamaterials with ultralow refractive index," J. Opt. Soc. Am.B/Vol.20, No.12 (December 2003)

[5] D. R. Smith and N. Kroll, "Negative refractive index in left-handed materials," Phys. Rev. Lett. 85, 2933 (2000)

[6] J. B. Pendry, A. T. Holden, W. J. Stewart and I. Youngs, "Extremely-Low-Frequency Plasmons in Metallic Mesostructures," Phys. Rev. Lett. 25, 4773 (1996)

[7] D. R. Smith, W. J. Padilla, D. C. Vier, R. Shelby, S. C. Nemat-Nasser, N. Kroll and S. Schultz, "Left-handed metamaterials," Photonic Crystals and Light Localization, ed. C. M. Soukoulis (Kluwer, Netherlands, 2000)

[8] D. R. Smith, J. J. Mock, A. F. Starr and D. Schurig, "Gradient index metamaterials," Physical Review E , 71, 036617 (2005)

[9] J. B. Pendry, D. Shurig and D. R. Smith, "Controlling electromagnetic fields," Science 312, 1780 (2006)

[10] T. J. Cui, D. R. Smith, R. Liu, "Metamaterials Theory, Design, and Application," Springer (2010)

[11] Molecular Expressions, National High Magnetic Field Laboratory (NHMFL) and the Florida State University Research Foundation (FSURF)

[12] en.wikipedia

[13] NASA

[14] IEEE Standard for Safety Levels With Respect to Human Exposure to Radio Frequency Electromagnetic Fields, 3 kHz to 300 GHz. IEEE C95. (1-2005)

[15] American National Standard for Safe Use of Lasers. ANSI Z136. (1-2007)

[16] F. T. Ulaby, "Fundamentals of Applied Electromagnetics," Prentice Hall 2011, ISBN-13: 978-0132139311 Edition: 6

[17] S. Cherukulappurath, Optics & Photonics Focus, Volume 13, Story 3 – (3/5/2011)

[18] D. R. Smith, D. C. Vier, T. Koschny, and C. M. Soukoulis, "Electromagnetic parameter retrieval from inhomogeneous metamaterials," Physical Review E - Statistical, Nonlinear, and Soft Matter Physics, vol. 71, pp. 036617/1-036617/11 (2005)

[19] CST of America®, Inc.

[20] S. M. Mansfield and G. S. Kino, "Solid immersion microscope," Appl. Phys. Lett. 57, 2615 (1990).

[21] Z. Lu, B. Camps-Raga and N. E. Islam, "Design and Analysis of a THz Metamaterial Structure with High Refractive Index at Two Frequencies," Physics Research International, vol. 2012, Article ID 206879 (2012)

[22] J. T. Shen, P. B. Catrysse and S. Fan, "Mechanism for designing metallic metamaterials with a high index of refraction," Phys. Rev. Lett. 94, 197401 (2005)

[23] A. Pimenov and A. Loidl, "Experimental demonstration of artificial dielectrics with a high index of refraction," Physical Review B, vol. 74, no. 19, Article ID 193102 (2006)

[24] Y. M. Shin, J. K. So, J. H. Won, and G. S. Park, "Frequency-dependent refractive index of one-dimensionally structured thick metal film," Appl. Phys. Lett. 91(3), 031102 (2007)

[25] H. Shi, C. Wang, X. Wei and C. Du, "Plasmonics metamaterials of high refractive index at visible frequency," Metamaterials, 2008 International Workshop on, pp. 153- 156, 9-12 Nov. (2008)

[26] Wei, X., Shi, H., Dong, X., Lu, Y., and Du, C. "A high refractive index metamaterial at visible frequencies formed by stacked cut-wire plasmonic structures," Appl. Phys. Lett. doi:10.1063/1.3453477 (2010).

[27] J. Shin, J. T. Shen, and S. Fan, "Three-dimensional metamaterials with an ultrahigh effective refractive index over a broad bandwidth," Phys. Rev. Lett. 102, 093903 (2009)

[28] G. Kirchhoff, "Zur Theorie des Condensators," Monatsber.Akad. Wiss. Berlin, 144 (1877)

[29] G. J. Sloggett, N. G. Barton, and S. J. Spencer, "Fringing field in disc capacitors," J. Phys. A: Math. Gen, vol. 19, No.14, pp.2725–2736, Oct. (1986)

[30] M. Choi, S. H. Lee, Y. Kim, S. B. Kang, J. Shin, M. H. Kwak, K.-Y. Kang, Y.-H. Lee, N. Park, and B. Min, "A terahertz metamaterial with unnaturally high refractive index," Nature470(7334), 369–373 (2011)

[31] Y. Yuan, C. Bingham, T. Tyler, S. Palit, T. H. Hand, W. J. Padilla, N. M. Jokerst and S. A. Cummer, "A dual-resonant terahertz metamaterial based on single-particle electric-field-coupled resonators," Applied Physics Letters 93, 191110 (2008)

[32] Y.Yuan, C.Bingham, T. Tyler, S. Palit, T. H. Hand, W.J.Padilla, D.R.Smith, N.Marie Jokerst and S.A.Cummer, "Dual-band planar electric metamaterial in the terahertz regime," Vol.16, No.13 (2008)

APPENDIX

Code for parameter retrieval:

```
s11=s11real(:,2)-1i*s11imag(:,2);
s21=s21real(:,2)-1i*s21imag(:,2);

c=3*10^8;

d=5*10^(-6);

f=s11real(:,1)*10^12;
lamda=c./f;
k=2*pi./lamda;

s21t=(exp(0*1i.*k.*d)).*s21;

z1=+sqrt(((1+s11).^2-s21t.^2)./((1-s11).^2-s21t.^2));
z2=-sqrt(((1+s11).^2-s21t.^2)./((1-s11).^2-s21t.^2));

z=[];
[p,q]=size(f);

for t=1:1:p

   if (real(z1(t,1))>0)||(real(z1(t,1))==0)
       z(t,1)=z1(t,1);
   else
     if (real(z2(t,1))>0)||(real(z2(t,1))==0)
       z(t,1)=z2(t,1);
     end
end
end

m=0;

z=real(z)+1i*imag(z);

realn=real(acos((1-(s11.^2-s21t.^2))./(2.*s21t))./(k.*d))+2*pi*m./(k.*d);
imagn=imag(acos((1-(s11.^2-s21t.^2))./(2.*s21t))./(k.*d));

n=realn+1i.*imagn;

epsilon=n./z;

u=n.*z;

figure(1), plot(f,real(n),'r',f,imag(n),'--r'),title('index n');
hold on
figure(2), plot(f,real(z),'r',f,imag(z),'--r'), title('impedence');
hold on
figure(3), plot(f,real(epsilon),'r',f,imag(epsilon),'--r'), title('permittivity');
hold on
figure(4), plot(f,real(u),'r',f,imag(u),'--r'),title('permeability');
hold on
```